



investigate the role of pauses and backtracks during transcription elongation. With this, important insights could be obtained about transcription fidelity and its regulation using transcription factors. Moreover, information about the nucleosomal barrier and its effect on transcription elongation come from AFM as well as optical tweezer experiments. Also, most recently, single-molecule studies have advanced to the complex environments of living cells, obtaining quantitative information about single-molecule events in real live situations.

While the field of single-molecule transcription is still at its early stages, already a number of excellent review articles have appeared.<sup>18–22</sup> Therefore, rather than attempting to give a complete overview of all experiments and results obtained until today, we want to focus on some recent results, while at the same time show the enormous potential offered by the specific capabilities of different methods. Many of the described experiments require sophisticated single-molecule methodologies, and we will first provide a brief overview of these techniques that are revolutionizing the transcription field.

## 2. SINGLE-MOLECULE METHODOLOGY

### 2.1. Single-Molecule Fluorescence

Single-molecule fluorescence microscopy and spectroscopy have become extremely powerful techniques for molecular and cellular biology;<sup>23–28</sup> however, for their implementation significant technical obstacles had to be overcome. Detecting the fluorescence signal from just a single chromophore is the ultimate sensitivity limit in fluorescence spectroscopy, and therefore strong precaution had to be taken to minimize background fluorescence and stray light. Nevertheless, pioneering work by Moerner and Kador<sup>29</sup> and Orrit and Bernard<sup>30</sup> at low temperature, as well as by Yanagida at room temperature,<sup>31</sup> made the first demonstrations of single-molecule fluorescence detection possible. Since then, single-molecule fluorescence methods have been applied to study nucleic acid dynamics,<sup>32</sup> protein movement on DNA,<sup>33,34</sup> molecular motors,<sup>35</sup> enzyme dynamics,<sup>36–38</sup> and protein folding.<sup>39,40</sup> Furthermore, it has been used to determine the stoichiometry of complexes,<sup>41,42</sup> for single-molecule sequencing,<sup>43,44</sup> and in live cell experiments.<sup>45,46</sup>

In a typical single-molecule fluorescence experiment, the molecule of interest is labeled with a single fluorophore at either arbitrary or specific sites on the molecule depending on the particular application. In some instances, the overall position of the labeled molecule should be monitored such as in experiments tracking single molecules,<sup>47–50</sup> measuring diffusion times,<sup>51</sup> colocalization with other molecules,<sup>52</sup> or cross-correlation of different molecules.<sup>53</sup> For these experiments, the molecule can be labeled at any arbitrary position, which does not interfere with its function. However, oftentimes the fluorophore is used as a local probe for the structure and dynamics of the molecule of interest, and therefore site-specific labeling approaches are required.<sup>54–62</sup>

There are generally two different single-molecule fluorescence experimental modes: in solution measurements and immobilization. For in solution measurements, the molecule of interest is studied in solution using confocal microscopy, where the observation time is limited by the diffusion of the molecule through the confocal volume. Alternatively, the molecule is immobilized to investigate longer time trajectories of the single-molecule fluorescence.<sup>63–66</sup> In experiments with immobilized molecules, one of the main limitations is the photostability of

the fluorophore. Therefore, considerable experimental effort has been made to optimize the photostability of dye molecules,<sup>67–69</sup> as well as to use specialized buffer solutions for optimizing the amount of photons emitted by the fluorophores prior to photobleaching.<sup>70–72</sup> Some alternatives to single dye molecules have also been proposed, small semiconductor particles called quantum dots,<sup>73–75</sup> small metal clusters,<sup>76</sup> or defect centers in diamond.<sup>77</sup> However, blinking of these point emitters, their relatively large size, and problems in site-specific attachment are currently limiting the utility of these alternative labeling methods. More recently, the control of fluorophore blinking has become important for biological applications, because turning fluorophores on and off is used in super-resolution optical microscopy experiments such as STORM and PALM.<sup>78–87</sup>

**2.1.1. Single-Molecule FRET.** One of the most prominent single-molecule fluorescence techniques is single-molecule Förster resonance energy transfer (smFRET, Figure 1).<sup>88–93</sup>

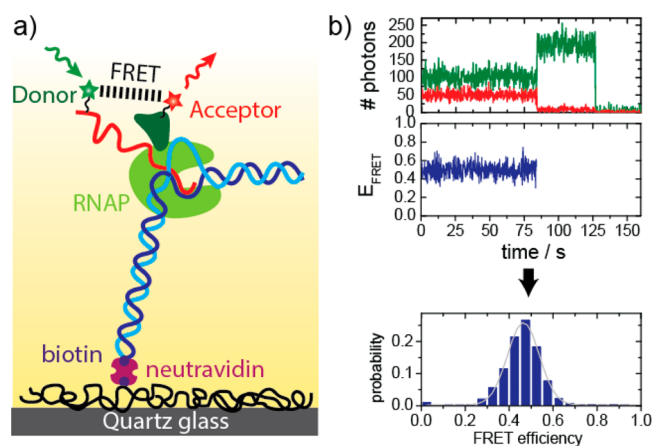


**Figure 1.** Single-molecule FRET experiments. (a) Schematic of smFRET experiments on transcription elongation complexes. An elongation complex is performed in solution and diluted to nanomolar concentrations. To investigate complexes for an extended period of time, they are immobilized on a surface. To this end, silanized fused silica slides are passivated using, for example, a PEG layer. Neutravidin molecules are then attached to the surface, and transcription elongation complexes are bound using, for example, biotinylated DNA. The complexes are labeled with two dye molecules, a donor and an acceptor, which form a smFRET pair. Excitation of the donor fluorescence (e.g., using a total internal reflection microscope) leads to energy transfer. Both the fluorescence signals of donor and acceptor are then detected simultaneously. (b) Time trajectory of smFRET and histogram of smFRET efficiencies. The detected donor fluorescence (green), acceptor fluorescence (red), and calculated smFRET efficiency (blue) are shown as a function of time. After  $\sim 80$  s, photobleaching of the acceptor molecule leads to a stepwise increase in the observed intensity of the donor. After  $\sim 120$  s, photobleaching of the donor occurs. The FRET efficiency is calculated by using this intensity data. From this efficiency as a function of time, the distribution of observed smFRET efficiency is computed (lower panel).

Here, two fluorophores, the fluorescence donor and the fluorescence acceptor, are attached to a molecule of interest. The amount of energy that is transferred from the donor to the acceptor depends on the relative donor fluorescence quantum yield, the overlap integral of the donor emission and the acceptor excitation spectra, the index of refraction, and most importantly the distance between the two dye molecules. As

theorized by Förster,<sup>94</sup> and first experimentally verified by Haugland and Stryer,<sup>95</sup> the efficiency of energy transfer,  $E$ , depends on the distance to the sixth power, and varies on length scales of the size of single macromolecules. For this reason, FRET has also been termed a molecular ruler. At the single-molecule level where photobleaching is observed frequently, the simultaneous digital change in fluorescent intensity of both donor and acceptor is a good indicator of smFRET (Figure 1b). Furthermore, photobleaching of the acceptor can be used to calculate an important correction factor, the  $\gamma$  factor, which accounts for differences in detection efficiencies of donor and acceptor as well as the ratio of their fluorescence quantum yields.<sup>96</sup> Because smFRET can provide time-resolved data on the immobilized single molecules, it has been used frequently to monitor conformational changes of biomolecules.<sup>97–99</sup> In measurements of molecules diffusing through the confocal volume, where observation times are too short to observe extended fluorescence trajectories, information about conformational dynamics has been obtained indirectly using statistical analysis.<sup>100–103</sup>

Even though changes in the observed smFRET efficiencies are good indicators of distance changes, obtaining quantitative distance information requires substantial experimental effort to determine all variables defining the Förster distance.<sup>66,104–106</sup> However, once quantitative information is extracted from smFRET experiments, the measurement of a whole network of distances can be used to obtain structural information as will be discussed in the next section.<sup>107–112</sup>

**2.1.2. The Nano-Positioning System (NPS).** Many biological complexes consist of numerous subdomains, and knowing the structure of an entire complex is important for its complete functional understanding. However, the relative position of each subdomain is oftentimes difficult to determine. Possible reasons for the inability to determine the position or structure of a subdomain by standard structural biology methods are the transient nature of cofactor binding to a larger complex, or the existence of flexibility in the subdomain. Here, smFRET measurements provide a useful alternative. By measuring at least three different distances from positions known from a crystal structure to the unknown position of interest, one can in principle infer the unknown position by simple triangulation.<sup>113</sup> However, because every measured smFRET distance is associated with an intrinsic error (Figure 2), finding the most likely position and estimating the absolute uncertainty becomes difficult. To this end, the Nano-Positioning System (NPS) was developed.<sup>109</sup> In NPS, the unknown position of a dye molecule, called antenna, is determined by a set of smFRET distance measurements to known positions called satellites (in analogy to the global positioning system). The smFRET distance measurements contain uncertainties due to attachment of dye molecules via flexible linkers, unknown relative orientations of the dye molecules, as well as measurement errors. To obtain quantitative information, these uncertainties can be accounted for by a probabilistic bayesian parameter estimation approach. As a result, the complete three-dimensional position information in the form of a probability density function, the so-called posterior, is obtained. To get an intuitive picture of the experimental uncertainty, the position is visualized by credible volumes, defined as the smallest volume that encloses a certain probability for the dye position, for example, 68% for one standard deviation. More recently, the NPS was expanded to analyze networks of positions, include FRET anisotropies, and perform distance restrained docking.<sup>110</sup>

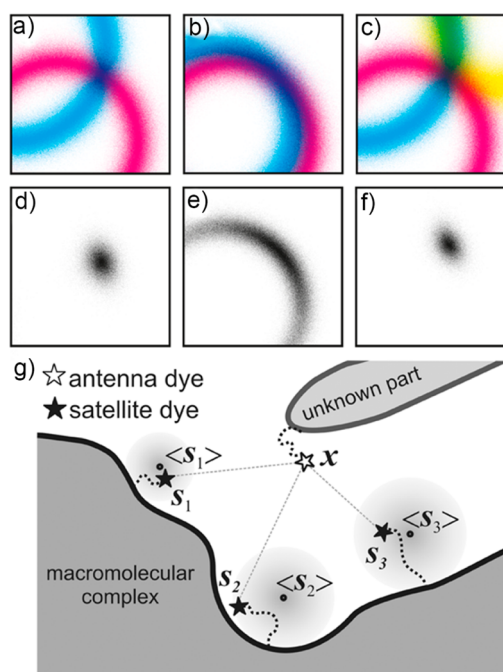


**Figure 2.** Triangulation uncertainties and the Nano-Positioning System. (a–f) Using smFRET data to derive distance information, one obtains the most likely distance together with an uncertainty. With respect to one dye molecule, the other dye molecule is then known to sit at the surface of a fuzzy sphere, or in 2-D on a fuzzy circle with the fuzziness describing the uncertainty. Here, the information of two measurements (a,b) or three measurements (c) is shown. (d–f) From the overlay of the fuzzy circles, the resulting probability density can be computed (gray clouds). In addition to the uncertainty of each measurement, both the geometry of the measurements as well as the number of measurements performed determine the final shape and size of the uncertainty. (g) Idea of the NPS system. The position of an unknown part within a biological structure is determined through a set of smFRET measurements. To this end, smFRET is measured between a dye molecule attached to a known position (satellite,  $S$ ) and another dye molecule attached to an unknown position (antenna,  $X$ ). Note that the position of the attachment point of the satellite is known (e.g., from a crystal structure), but not the position of the satellite itself (gray clouds) because the dye molecule is generally attached to the known position through a flexible linker. The information from at least three smFRET measurements is then used to compute the position of the antenna dye as illustrated in (a)–(f).

Recently, another smFRET-based structural analysis tool, FRET restrained high-precision structural modeling (FPS), was developed.<sup>107</sup> In addition to a different treatment of the linker to which the dye molecule is attached, FPS includes molecular dynamics (MD) simulations. As a consequence, this method may be limited to relatively small complexes. Both of these smFRET-based structural methods have shown promising applications in structural biology. In particular, the NPS was used to analyze initiation and elongation complexes of the eukaryotic RNA polymerase II, on which we will elaborate in the applications section (sections 3–8) of this Review.

## 2.2. Single-Molecule Force Spectroscopy

Mechanical forces underlie nearly all cellular processes, in particular those that involve directed movement, such as transport or polymerization.<sup>114</sup> Multiple methods have been developed to measure forces directly and at the level of single molecules including mechanical levers,<sup>115–118</sup> optical tweezers,<sup>119–122</sup> and magnetic tweezers.<sup>123,124</sup> We will focus on

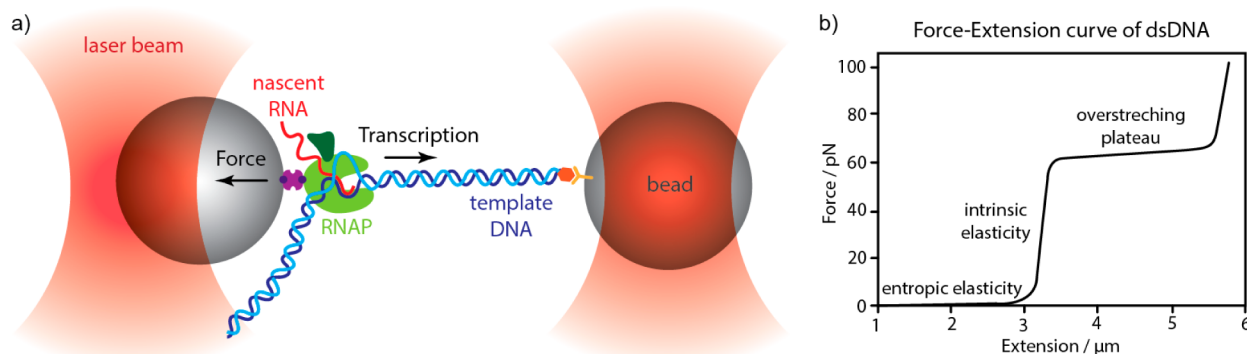


**Figure 3.** Single-molecule transcription studied by optical tweezers. (a) Schematic showing the experimental geometry for transcription elongation experiments studied using optical tweezers. Two beads are held in two optical tweezers in a dumbbell geometry. The RNA polymerase is attached to one of the beads and the end of the DNA to the other bead. In the shown geometry, the downstream DNA is attached, so that the polymerase is moving against the exerted force. Thus, the enzymatic reaction is slowed by the external force. The amount of force applied can be calculated by measuring the displacement of the beads from the center of the optical traps. For most experiments, one is operating in the linear regime, where the displacement is proportional to the force. To calculate the movement of the polymerase, one needs to account for both the stiffness of the optical trap as well as the force extension behavior of the DNA. (b) Force extension data for a single DNA molecule. The data can be described nicely by the extended worm-like chain model for forces up to  $\sim 40$  pN. At about 60 pN, the DNA molecule changes its mechanical properties, the so-called transition of the canonical B-DNA to S-DNA. However, experiments on RNA polymerases are typically performed at forces below 30 pN, so that the extended worm-like chain model can be used.

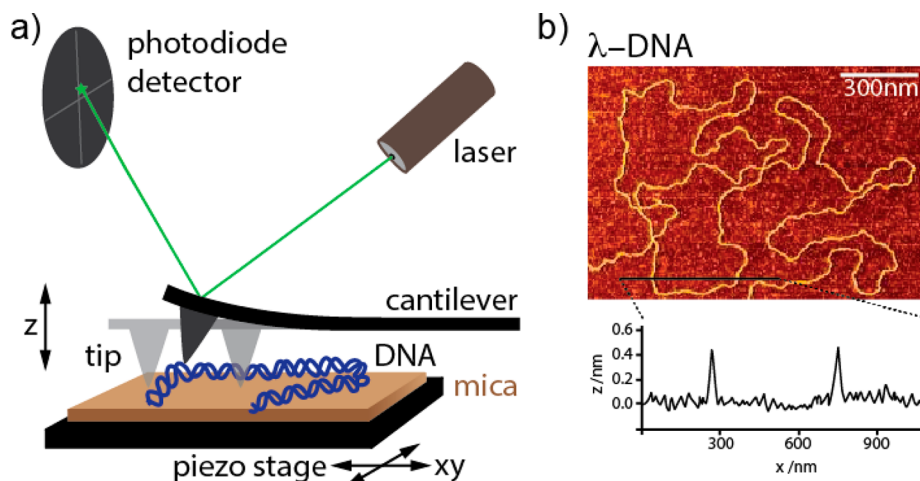


**Figure 4.** AFM imaging of biomolecules. (a) Schematic of AFM imaging of a DNA molecule. A DNA molecule attached to mica is raster-scanned underneath the tip of an AFM cantilever. By monitoring the displacement of the tip and applying a feedback mechanism, one can work at a constant force. If the tip encounters an obstacle such as the DNA molecule, the feedback circuit will retract the tip. Thus, the movement of the tip will reflect the inverse of the topography of the sample. For accurate mapping of the topography, one will need to deconvolute with the tip shape. (b) AFM image of a  $\lambda$ -phage DNA molecule adsorbed to mica and imaged in air. The black line marks the position of a cross-section, which is shown below. The topography of the DNA molecule is clearly visible in this cross-section. However, the height of the molecule is lower than one would expect, due to the applied force, the fact that the molecule is adsorbed, and due to the fact that the image is taken in air rather than in fluid environment.

optical tweezers in this Review because most experimental force spectroscopy experiments on RNA polymerases have employed this technique.

Light changes its momentum upon entering a medium with different index of refraction. Because of the physical law of momentum conservation, the medium also experiences a change in momentum. This phenomenon is harnessed in optical tweezers, where small dielectric objects such as micrometer-sized beads made out of polymer or glass are trapped in the maximum of the light intensity distribution of a focused laser beam. If the bead moves out of the center position, the laser exerts a force onto the bead that draws it back into the maximum of the light intensity distribution.<sup>125–128</sup> Therefore, optical tweezers can be used to manipulate and detect displacements with very high spatial

sensitivity (down to 1 Å),<sup>129</sup> and measure extremely low forces (down to fN).<sup>130</sup> In addition, biological molecules, such as an RNA polymerase transcribing along a DNA molecule, can be held in place by two optical tweezers (Figure 3). This so-called dumbbell design effectively shields the biological system from mechanical noise in the laboratory, so that stepping behavior of the enzyme in the subnanometer range can be observed with high accuracy.<sup>131–133</sup>

A typical optical tweezers experiment of RNA polymerase transcription starts with a calibration of the tweezers, which is commonly done for each trapped bead using a power-spectrum analysis.<sup>134,135</sup> A single transcribing complex is then attached between two beads using modified polymerase (e.g., biotinylated) and modified DNA (e.g., digoxigenin) (Figure 3). The modification on the DNA can be either downstream of the

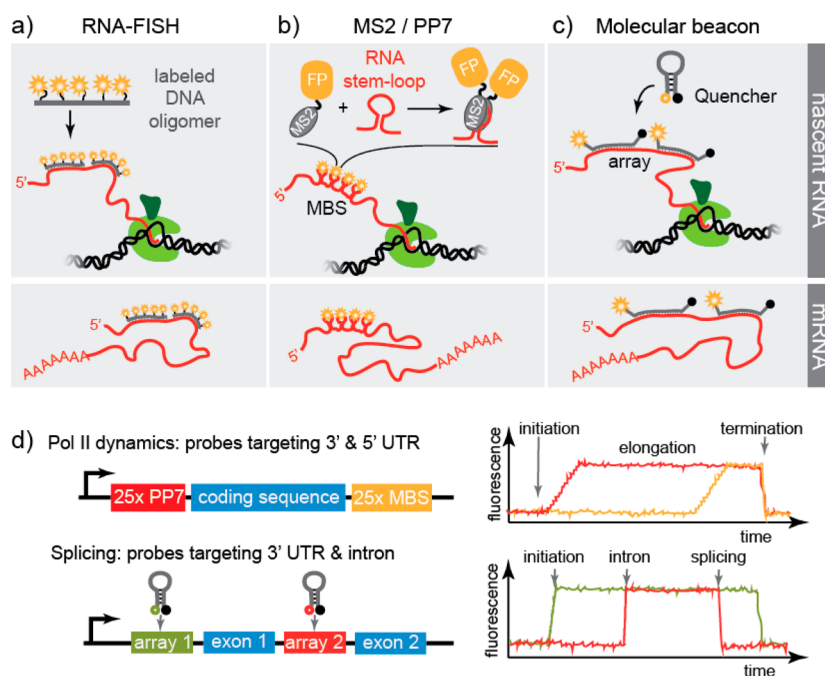


**Figure 5.** Methods of imaging single-molecule transcription in vivo. (a–c) Schematics of current methods, which are based on visualizing single RNA molecules at the site of active transcription (nascent RNA, top) as well as mature mRNA in the cytosol (bottom). RNA polymerase, green; DNA, black; RNA, red. (a) RNA-FISH uses DNA oligomers that are fluorescently labeled at multiple positions and complementary to the gene of interest. Hybridization leads to labeling of the RNA, and the presence of multiple fluorophores ensures a signal high enough to be detected above noise. (b) In the MS2/PP7-FP technique, a cassette encoding several repeats of the MS2 (or PP7) coat protein binding site (MBS) is genetically introduced into the untranslated region of the gene of interest. As the cassette is transcribed by the RNA polymerase, RNA stem loops form and recruit the MS2/PP7-FP fusion protein that is constitutively coexpressed and serves as fluorescent tag (FP = fluorescent protein). (c) Molecular beacons are single-stranded DNA probes that become fluorescent only upon hybridization. Hence, individual RNA molecules containing tandemly repeated sequences (signal amplification) can be fluorescently detected and tracked throughout the cell. (d) Schematic of methodological approaches to study the dynamics of initiation, elongation, termination, and cotranscriptional splicing in single living cells on the single-molecule level. Top panels: Dependent on the position of the inserted MBS cassette (5'UTR versus 3'UTR), the gene construct is sensitive either to whole transcription cycles (5'UTR, fluorescent signal increases stepwise shortly after initiation) or only to late events in the lifetime of the nascent RNA (3'UTR, fluorescent signal detectable only after elongation, shortly before termination of transcription). By combining time-lapse data from 5'UTR and 3'UTR constructs, it is possible to determine kinetic rates of initiation and elongation. Bottom panel: Two distinctly labeled sets of molecular beacons designed against the 3'UTR as well as an intronic region of the gene of interest can be used to study the dynamics of cotranscriptional splicing and its effect on transcription elongation. Co-localization of the fluorescent signal of 3'UTR and intronic region is lost upon splicing.

RNA polymerase for experiments where the polymerase has to overcome an opposing force, or upstream of the polymerase, such that force is assisting the polymerase during transcription. The force–extension behavior of DNA molecules is well studied<sup>136,137</sup> and can be best described by an extensible worm-like chain model.<sup>138</sup> Therefore, changes in the observed force due to the action of the polymerase can be related to the movement of the polymerase on the DNA using the extensible worm-like chain model, and the precise position of the polymerase on the DNA template can be determined.<sup>139</sup>

### 2.3. Imaging of RNA Transcription

Imaging RNA polymerases during individual transcription events using optical or atomic force microscopy can provide kinetic as well as structural insights into the transcription process. To follow the movement of the RNA polymerase on DNA by optical microscopy, either the polymerase itself is labeled using a bead in a so-called tethered particle assay,<sup>140</sup> or a fluorophore is attached to the DNA molecule. We will present applications of the tethered particle assay to transcription elongation in section 3.2 of this Review. Besides optical microscopy, atomic force microscopy is a very important technique to image the RNA polymerase and DNA during transcription.<sup>141–143</sup> In an AFM, a mechanical cantilever is

scanned over a substrate, and by optically measuring the deflection of the cantilever, the topography of the sample is recorded (Figure 4). Typically complexes are assembled in solution and then immobilized on flat substrates such as freshly cleaved mica for imaging.<sup>144</sup> Depending on the interaction strength between surface and transcription complexes, by means of AFM one can either study the equilibrium of the complexes or trap different kinetic states.<sup>145</sup> Using AFM imaging, Bustamante and co-workers first described the bending of DNA during transcription initiation and elongation.<sup>146</sup> By measuring the position of the polymerase on the DNA molecule, and comparing the length of DNA flanking the polymerase during various phases of transcription to the length of free DNA in the absence of polymerase, information about the overall architecture of transcription complexes and interactions between the RNA polymerase and the DNA template could be extracted.<sup>147,148</sup> Most previous AFM experiments on transcription complexes were performed in air with the drawback that the imaged complexes exist in a non-natural, fixed conformation. In contrast, when AFM imaging is performed in solution, one is able to capture conformational changes during transcription at the level of a single complex.<sup>149,150</sup> Such kinetic experiments, however, have been

hampered by the relatively slow temporal resolution of the AFM microscope.

More recently, the speed with which AFM images can be acquired has been revolutionized by the heroic efforts of Ando and co-workers.<sup>151</sup> With such ultrafast AFM microscopes, stepping of myosin V motor proteins<sup>152</sup> and binding of ATP molecules to A1-ATPase<sup>153</sup> could be resolved at rates of about 10 frames/s. It is only a matter of time until this high speed AFM imaging will be applied to transcription.

#### 2.4. Imaging Transcription in Single Cells

As a result of fast advances in live-cell imaging technologies in recent years, it has become possible to apply single-molecule fluorescence microscopy to single cells and directly observe individual transcription events in single living cells. In vivo single-molecule studies of transcription are mainly based on the fluorescent detection of single mRNA molecules, which has been achieved using several different labeling strategies. In general, single mRNA molecules have to be labeled with multiple copies of a fluorophore to amplify the fluorescent signal to a detectable level.<sup>20,154</sup>

The first demonstration of single mRNA detection, which was achieved by Robert Singer and co-workers,<sup>155</sup> was based on single RNA fluorescence in situ hybridization (mRNA-FISH). This technique uses synthetic DNA oligomers fluorescently labeled at multiple positions and complementary to the mRNA of interest (Figure 5a). The DNA probes are added to paraformaldehyde-fixed cells, and hybridization leads to labeling of the RNA.<sup>155,156</sup> In this way, single mRNAs in the cytoplasm as well as nascent mRNAs at the site of active transcription can be detected. mRNA-FISH has now been applied to a variety of systems ranging from bacteria and yeast to mammalian cells and tissue.<sup>157–161</sup> One advantage of this methodology is the ability to observe endogenous transcripts without the need of genetic engineering. In addition, the transcripts of several genes can be simultaneously detected if probes targeting different genes are labeled with fluorophores emitting in a different spectral range. Moreover, the total number of mRNAs of the gene of interest per cell can be counted, and hence the probability distribution of transcription can be extracted. A major disadvantage is the requirement to fix the cells prior to mRNA detection, because only snapshots of the highly dynamic process of transcription can be obtained.

The second labeling strategy exploits the high affinity of the bacteriophage MS2 coat protein (or the homologous bacteriophage PP7 coat protein) for short RNA sequences in the bacteriophage genome that form specific stem-loop structures.<sup>162,163</sup> A cassette encoding several repeats of the MS2 (or PP7) coat protein binding site (MBS) is genetically introduced into the untranslated region (UTR) of the gene of interest, and cells are engineered to constitutively express a MS2/PP7-fluorescent protein (FP) fusion construct. As the cassette is transcribed by Pol II, RNA stem loops form and are bound by the MS2/PP7-FP fusion constructs that therefore serve as fluorescent tags (Figure 5b). Hence, nascent RNA as well as cytosolic mRNA can be detected. The MS2-FP technique was originally developed using tandem gene arrays, where multiple copies of a reporter were introduced at a certain genomic locus,<sup>164,165</sup> and has subsequently been modified for single copy insertions to study transcriptional dynamics of single alleles<sup>166,167</sup> as well as for the study of endogenous genes in yeast and even in a knock-in mouse.<sup>162,168</sup> Very recently, both PP7- and MS2-based mRNA labeling were combined in

yeast such that in a two-color experiment, the beginning and the end of a nascent RNA molecule could be individually detected, and Pol II transcription dynamics could be directly observed. Moreover, transcription of the two alleles of the same gene could be observed simultaneously in a two-color experiment.<sup>162,169</sup>

The MS2/PP7-FP method has been used extensively to study transcription in a variety of systems,<sup>162,164,168,170–172</sup> and is generally assumed to have low interference with the transcription process. The major advantage of the MS2-FP technique is the possibility to follow transcription in real-time in living cells and even living organisms, because fixation of cells is not required. As a consequence, kinetics of the transcription process such as the rate of transcription initiation, elongation, and termination can be studied in vivo (Figure 5d). A disadvantage of this method is that to study the transcriptional dynamics of a gene in the context of its endogenous chromatin environment, an MBS cassette has to be introduced into the endogenous locus. Traditionally, this has required the use of homologous recombination techniques only applicable in a few systems, such as bacteria, yeast, and embryonic stem cells. However, due to the fast development of new genome engineering methods such as TALENs<sup>173</sup> and the CRISPR system,<sup>174</sup> the targeted introduction of an exogenous DNA sequence of interest into a specific genomic locus is becoming increasingly feasible for other systems, such as tissue culture and zebrafish.

A third method to label mRNA in vivo is based on molecular beacons,<sup>175,176</sup> that is, single-stranded DNA probes that contain a fluorophore–quencher pair as well as complementary sequences at its ends. Free in solution, the oligomer forms a hairpin, which brings the fluorophore in close proximity to the quencher such that its fluorescence emission is quenched. Only upon hybridization to the target sequence, the probe becomes fluorescent due to an increase in distance between the fluorophore–quencher pair (Figure 5c). Molecular beacons have been used to detect individual RNA molecules containing tandemly repeated target sequences in living mammalian cells.<sup>177,178</sup> Similar to the MS2-FP system, this method holds the great advantage of being applicable to real-time studies of transcription in living cells (Figure 5d).

Apart from directly imaging mRNA, information about the dynamics of mRNA coding for a fluorescent protein can be inferred indirectly from the fluorescent or luminescent signal of that reporter protein. To be able to relate the protein signal to the abundance of the mRNA intermediate, the reporter protein has to be short-lived so that only newly synthesized proteins emit a fluorescent or luminescent signal.

In addition to labeling mRNA to study transcription in vivo, protein factors controlling the transcription process such as transcription factors or the RNA polymerase itself can be labeled via fusion to a fluorescent protein. When used in combination with the MS2-FP or molecular beacon technique, colocalization of labeled proteins and nascent RNA can provide information about the presence of transcription factors at the site of active transcription. A recent technological advance applied reflected light sheet microscopy to study the dynamics of transcription factor binding in live mammalian cells.<sup>179</sup> The thin light sheet allows for an improved signal-to-noise ratio as compared to standard illumination schemes and enables imaging of single fluorescent proteins with high temporal resolution. Therefore, this technique will enable single-

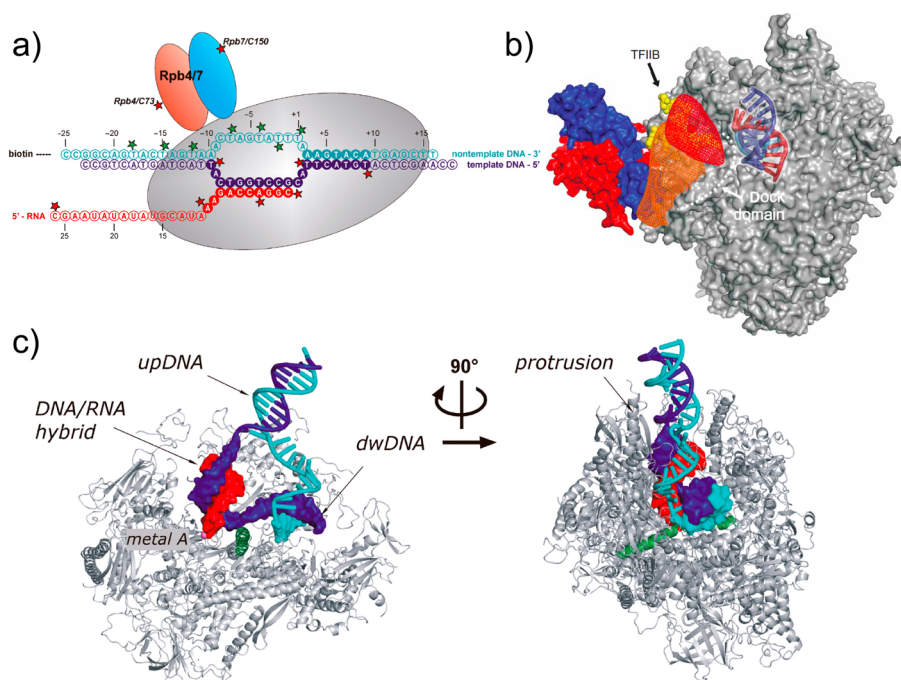


**Figure 6.** Nanopositioning studies of Pol II transcription elongation. (a) Schematic of the nucleic acid scaffold used for the NPS studies of Pol II transcription elongation. Elongation complexes were assembled using an 11nt mismatch between the template and the nontemplate strand together with an RNA primer. Solid circles refer to bases whose position is known from X-ray studies. Open circles refer to unknown positions. Labeling positions are marked with red stars for the satellite positions and green stars for antenna positions. Satellite positions on Rpb4/7 were introduced using single cysteine mutants of the recombinant protein that was combined with endogenous 10 subunit core polymerase. For surface attachment of the complexes, the 5'-end of the nontemplate strand was marked with biotin. (b) NPS localization of the position of a dye molecule attached to the 5' end of a 26nt RNA molecule.<sup>109</sup> The localization is shown in the absence (red) and presence (orange) of transcription initiation factor TFIIB. Displayed are the most likely positions (spheres) together with a mesh showing the credible volume contoured at 68% to get an intuitive understanding of the accuracy of the model. (c) The position of the nontemplate and upstream DNA in a Pol II elongation complex revealed through NPS experiments.<sup>108</sup> NPS localization of seven different positions along the nontemplate DNA (shown in (a)) allowed to build a model for the pathway of the nontemplate strand, as well as of the position of the upstream duplex DNA. (a),(b) Adapted from ref 109 with permission from Nature Publishing Group, copyright 2008. (c), (d) Adapted from ref 108 with permission from Oxford University Press, copyright 2009.

molecule in vivo studies of transient transcription factor binding during initiation, elongation, pausing, or termination.

Moreover, fluorescence correlation spectroscopy (FCS) as well as fluorescence recovery after photobleaching (FRAP) can be used to extract diffusion and binding dynamics of transcription factors as well as of the RNA polymerase on the time scale of milliseconds (FCS) to seconds (FRAP).<sup>162,180</sup>

### 3. TRANSCRIPTION ELONGATION

#### 3.1. Structural Studies

X-ray structural analysis has yielded detailed information about the structure of the RNA polymerase as well as of RNA polymerase elongation, pausing or backtracking complexes. Nevertheless, the structures of parts of these complexes such as the nascent RNA remain unknown due to their flexibility and inherent mobility. In contrast to traditional structural methods, smFRET experiments in combination with Nano-Positioning System (NPS) analysis allow for the structural investigation of flexible complexes by direct visualization of single transcription complexes in real time. This approach was used to close several gaps regarding the structure of the RNA polymerase II elongation complex. First, it was used to determine the position of nascent RNA exiting the polymerase (Figure 6a,b). In these experiments, elongation complexes were formed by using nucleic acid scaffolds containing an 11-nucleotide mismatched region of template and nontemplate strands, as

well as RNA primers of varying lengths.<sup>109,113</sup> As a result, the RNA was shown to leave the polymerase through the previously proposed RNA exit channel and follow a path across the dock domain. Interestingly, crystal structures of TFIIB–Pol II complexes show that TFIIB also binds to the dock domain of the polymerase, and indeed, addition of TFIIB to the elongation complexes in the smFRET experiments diverted the RNA path toward the polymerase stalk (Rpb4/7), a position that was previously observed in cross-linking experiments.<sup>181</sup>

In addition to the pathway of the nascent RNA, smFRET experiments and NPS were used to build a structural model of the pathway of the nontemplate DNA in the elongation complex<sup>108</sup> (Figure 6c) as well as that of the upstream DNA, which had previously only been examined by AFM experiments.<sup>146</sup> The path of the nontemplate DNA was found to be determined by several motifs on the surface of the RNA polymerase II previously identified in biochemical experiments: fork loop 2, the rudder, parts of the protrusion domain, as well as fork loop 1.

#### 3.2. Enzyme Translocation

One fundamental goal of single-molecule experiments has been to follow transcription of a single RNA polymerase in real time, such that the kinetics of the transcription process become directly observable. The first single-molecule experiments that were able to directly observe transcription used a tethered

particle motion assay on an optical microscope.<sup>140,182</sup> In this assay, the RNA polymerase is immobilized on the microscope slide, and a DNA template is translocated by the polymerase. The movement of DNA is visualized by the motion of a 40 nm gold bead attached to one end of the DNA. A similar approach was used to track the movement of single RNA polymerases along immobilized DNA.<sup>183</sup> Harada et al. extended the tethered particle assay by the use of an asymmetric particle, which allowed them to measure the rotation of DNA during translocation by the immobilized RNA polymerase.<sup>184</sup> These experiments showed that the RNA polymerase tracks the helicity of the DNA during transcription, because the translocated DNA was observed to rotate counterclockwise as viewed from the polymerase.

Already in the 1990s, optical tweezers were used to study RNA polymerase transcription.<sup>170,185–188</sup> The RNA polymerase was observed to be able to transcribe against an obstructive load, thereby converting chemical energy into a mechanical force, which shows that it constitutes a molecular motor.<sup>185</sup> Moreover, force exerted by optical tweezers on the T7 RNA polymerase was shown to act as a competitive inhibitor, slowing the movement of the enzyme.<sup>189</sup> However, it took a whole decade of technical improvement until the ultimate goal could be reached: being able to track the movement of a single enzyme step by step.<sup>132</sup> Several important experimental developments such as the design of dumbbell optical tweezers,<sup>190</sup> the use of an all optical feedback mechanism,<sup>191</sup> a slow down of the enzyme due to limited nucleotide concentration, as well as the use of a helium atmosphere to reduce low frequency noise were all important steps in this technical tour de force.

The RNA polymerase performs the polymerization reaction by advancing one base at a time (Figure 7), independent of the mechanical load. Single steps of the enzyme are separated by waiting times, during which a new nucleotide is loaded into the active center cleft. The dwell times between steps are therefore dependent on nucleotide concentration, but the size of each individual step is not. Because stepping depends on nucleotide concentration, limiting one of the four nucleotides and observing the dwell times as a function of position allows one to determine the sequence of the DNA on the single-molecule level.<sup>192</sup> Much attention has been paid to the kinetic aspects of *in vitro* transcription.<sup>186,189,193–195</sup> The pause-free velocity was shown to depend on force as well as on nucleotide concentration. However, the mean observed velocity of  $\sim 20$  bp/s at high nucleotide concentration and low force was several fold lower than the maximum transcription velocity observed *in vivo*. Only recently, the presence of ammonium chloride was found to substantially increase the velocity of Pol II *in vitro* at low (or assisting) force and saturating nucleotide concentration, such that the *in vivo* velocity is approached.<sup>196</sup>

Using data from opposing and assisting force experiments as well as minimal schemes of the nucleotide addition cycle, Block and co-workers modeled the kinetic behavior of both the bacterial RNA polymerase (RNAP)<sup>132</sup> as well as the eukaryotic enzyme, RNA polymerase II (Pol II).<sup>196</sup> They found that the single-molecule data could be explained best by a model, in which NTP binding occurs either before or after the 1 bp forward translocation of the enzyme.<sup>21</sup> However, to test different kinetic schemes of the enzyme, it is important to remove transcriptional pauses from the recorded data, a task that is extremely difficult, in particular if translocation of the

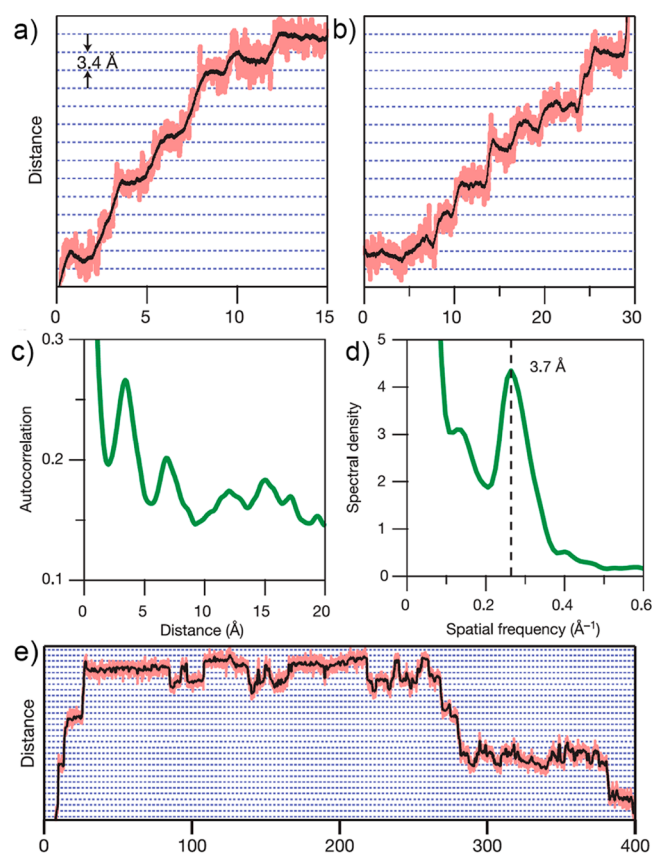


**Figure 7.** RNA polymerase stepping. (a and b) High-resolution optical tweezers data of RNAP transcription elongation showing individual single base pair steps. Experiments were done at low nucleotide concentration to reduce the rate of nucleotide incorporation to  $\sim 1$  Hz independent of sequence. An assisting force of  $\sim 18$  pN was applied to reduce experimental noise. Recorded data were filtered to 50 ms (pink) and 750 ms (black). (c) Autocorrelation function averaged over 37 runs showing peaks at 3.4 and 6.8 Å, indicative of the single base pair step size of the enzyme. (d) Computed power spectrum of (c) showing the spatial frequency corresponding to the single base pair stepping. (e) Backtracking of the RNAP observed at high opposing forces. When the polymerase experienced a high opposing force, transcription was sometimes interrupted by backtracks. Backtracking also occurs as a function of multiple 3.4 Å steps, indicating that forward and reverse motion follow a similar pathway. Some of the observed backtracks recovered spontaneously, while others led to a stall of the polymerase. Data representation is as in (a) and (b).<sup>132</sup> Adapted from ref 132 with permission from Nature Publishing Group, copyright 2005.

enzyme is slow and typical waiting times between translocation steps are comparable to pauses.

RNA polymerases show pauses in transcription even at high nucleotide concentration.<sup>186,194,197–201</sup> In the case of the bacterial enzyme, a large fraction of these pauses were reported to be ubiquitous, that is, sequence independent and without a concurrent backward movement of the polymerase. Backtracking of the enzyme, that is, a movement opposite to the direction of transcription, has also been observed frequently.<sup>190,202</sup> In fact, at high force, Pol II enters a dynamic equilibrium between forward translocation and backtracking, such that there is no longer any forward progress.<sup>203</sup> This kinetic force limit of  $\sim 10$  pN for the eukaryotic RNA polymerase is substantially lower than the thermodynamic stalling force observed for the bacterial enzyme. Recently, Grill

and co-workers developed a model, in which pausing is assumed to be caused by a backward diffusion of the polymerase, and they claim that most (if not all) of the experimentally observed pauses can be understood by the competition between backtracking and forward translocation.<sup>203,204</sup> The argument is based on the fact that the distribution of pauses follows a power law. As a consequence, an increase in experimental force simply shifts the pause distribution accessible to any experiment, given the experimental bandwidth and spatial resolution.

In addition to the above-discussed sequence-independent pausing, sequence-dependent pauses have been observed as well.<sup>139,199</sup> For Pol II, a statistical analysis of pause density and pause duration within AT- or GC-rich sequences showed an increased pause density and duration for AT-rich as compared to GC-rich sequences. Interestingly, treatment with RNase A, which digests the nascent RNA exiting the polymerase, eliminated this divergence, indicating that RNA secondary structure plays an important role in pausing even for the eukaryotic enzyme.<sup>205</sup>

### 3.3. Transcription Fidelity

One of the most important aspects in understanding the mechanistic principles of transcription is how the enzyme can, on the one hand, achieve fast and efficient polymerization and, on the other hand, have an enormous fidelity with an average error rate of only approximately 1 error in 100 000 bases.<sup>206,207</sup> Substantial information comes from structural studies investigating RNA polymerases in complex with different DNA lesions<sup>208,209</sup> as well as in backtracked states.<sup>210–212</sup> These studies indicate that two factors are important for fidelity: First, a motif close to the active center of the polymerase that undergoes structural changes during nucleotide addition, the trigger loop, and second, backtracking of the polymerase in combination with the action of transcription factors such as TFIIS,<sup>5,213</sup> TFIIF,<sup>214</sup> or Spt4/5<sup>215,216</sup> for the eukaryotic enzyme and GreA,<sup>217</sup> GreB, and NusG<sup>218</sup> for the bacterial polymerase,<sup>219</sup> respectively.

In mechanical experiments using optical tweezers, Block and co-workers investigated the pausing and backtracking of bacterial RNAP in the presence of GreA and GreB.<sup>190</sup> Both transcription factors decreased the observed frequency of long (>20 s) pauses. However, while GreB decreased the duration of long pauses and abolished backtracking, GreA had no effect on the duration of long pauses, and the average backtracked distance remained constant (or even increased slightly). The difference can be explained by the functional difference of these two factors. GreA is only able to cleave short RNA 3' overhangs, which are most likely not yet registered as a backtrack, whereas GreB can also cleave long RNA 3' overhangs, thus acting as a backtracking rescue factor. Similarly, in the case of the eukaryotic enzyme, TFIIS is able to cleave long RNA, and the addition of this transcription factor to Pol II in single-molecule optical tweezers experiments greatly reduces the probability of backtracking.<sup>203</sup> In fact, because backtracking determines the kinetic stalling of Pol II (see above), in the presence of TFIIS the stall force increased to ~20 pN, similar to the force that had been reported for the bacterial RNAP.<sup>186</sup> In contrast, the bacterial factor NusG was shown to increase the pause-free elongation rate as well as to decrease the frequency of short and long pauses of RNAP. Unlike GreB, NusG is believed to prevent the entry into a backtracked state, rather than rescue the polymerase once it is backtracked.

Structural, genetic, and computational studies have indicated that the trigger loop has an important function in the translocation of the RNA polymerase.<sup>10,17,220–225</sup> Single-molecule experiments recently explored the direct effect of specific point mutations within the trigger loop on velocity and fidelity of Pol II using either assisting or opposing forces.<sup>196</sup> Larson et al. investigated two different Pol II mutants: The first contained a single point mutation, E1103G, within a region of the trigger loop that becomes ordered in the crystal structure upon trigger loop closure, and the second mutant contained in addition to E1103G a mutation close to the binding site of the incoming NTP, H1085A. It should be noted that mutations at positions H1085 have severe effects, and Pol II with the single point mutation H1085A was shown to be lethal in yeast.<sup>226</sup> In the single-molecule experiments, Pol II E1103G had an increased catalytic rate and bound incoming nucleotides much tighter than the wild-type polymerase. Therefore, these data are in agreement with the notion that the trigger loop is important for catalysis. Because the  $K_D$  was also decreased, it is likely that E1103G increases the probability of the trigger loop to be in a closed conformation. In contrast, the additional mutation H1085A reversed some of the effects observed for E1103G: the catalytic rate of the double mutant was more than 3–6-fold below that of the wild-type enzyme, and the observed  $K_D$  was only slightly increased.

Even more interesting for the understanding of transcriptional fidelity are the effects of the mutants on Pol II pausing. Long pauses of Pol II, which are most likely due to backtracking, can be caused either by a stochastic effect or by the misincorporation of a wrong nucleotide. While the frequency of long pauses at nonlimiting nucleotide concentration was almost identical between wild-type and E1103 enzyme, a reduction of the concentration of one of the nucleotides led to a drastic increase in the pausing frequency of the mutant, but not of the wild-type Pol II. This suggests that the trigger loop mutant is more error prone, highlighting the role of the trigger loop in fidelity.<sup>196</sup>

## 4. TRANSCRIPTION IN THE PRESENCE OF NUCLEOSOMES

Experiments with a single polymerase and a single DNA molecule have helped our understanding of the molecular mechanism underlying transcription; however, they are not capable of describing the dynamics of transcription in the complex *in vivo* environment. In particular, in eukaryotes the presence of nucleosomes provides a completely different level of complexity.<sup>227,228</sup> In addition to understanding the function of chromatin marks<sup>229,230</sup> as well as active repositioning of nucleosomes by ATP-dependent nucleosome remodelers,<sup>231–234</sup> it is important to answer the question: what happens when an RNA polymerase encounters a nucleosome?

To describe how the RNA polymerases can bypass a nucleosome, one needs to understand nucleosome structure and dynamics. The structure of the nucleosome is well-known,<sup>235</sup> and more recently also the structure of a nucleosome on the 601 positioning sequence<sup>236,237</sup> oftentimes used in single-molecule experiments has been solved.<sup>238</sup> In a nucleosome, about 147 bp of DNA are wrapped in 1.65 turns of a flat, left-handed superhelix around an octamer of histone proteins. The minor groove of the DNA double helix faces inward and interacts with histones approximately every 10 bp, leading to 14 contact sites within 147 bp of nucleosomal DNA. Insights into nucleosome dynamics come from smFRET

experiments<sup>239–243</sup> as well as from mechanical experiments investigating the stability of nucleosomes using optical tweezers.<sup>244–249</sup>

Several previous mechanistic studies explored the effect of an RNA polymerase encountering a nucleosome<sup>250–256</sup> and reported that the presence of a nucleosome can drastically slow transcription. Moreover, factors that prevent or relieve pauses or backtracks were able to stimulate the observed transcription rates, indicating that pausing and backtracking plays an important role in transcription through nucleosomes. However, even though elegant in their approach, these studies lacked the direct insight into transcription kinetics at the level of a single molecule. It is expected that a roadblock like the nucleosome leads to distinct changes in the RNA polymerase kinetics, which have to be directly analyzed to understand the mechanism of transcription through a nucleosome.

Using optical tweezers, the laboratory of Carlos Bustamante was able to observe transcription of a single Pol II enzyme on a DNA containing a single nucleosome, positioned by the 601 sequence.<sup>257,258</sup> Assisting force was applied such that nucleosomal bypass by Pol II is facilitated. As compared to the behavior on free DNA, the dynamics of Pol II in the presence of the nucleosome were observed to change dramatically, and many long pauses and indefinite arrests were observed (Figure 8). Moreover, the frequency of an arrest

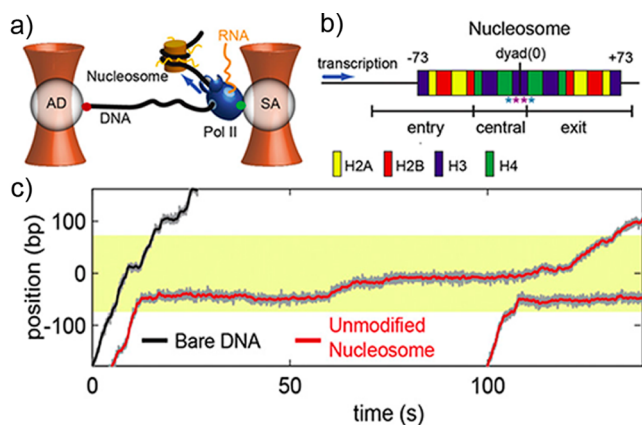


**Figure 8.** Transcription through the nucleosomal barrier. (a) Schematic of the single-molecule optical tweezers studies of Pol II bypassing a mononucleosome. A high-resolution dumbbell tweezers design operating in assisting force mode was used. Artificial, stalled elongation complexes were assembled<sup>202</sup> upstream of a mononucleosome localized on a 601 positioning sequence. (b) Schematic illustrating the nature of the nucleosomal barrier to Pol II transcription. A color-code for the histone proteins is used to map the histone DNA interaction sites along the DNA sequence. Positions of the Sin mutants are indicated by small stars. (c) Comparison of Pol II on bare DNA (black) and unmodified histones (red). While Pol II generally passes through the 601 sequence on bare DNA (approximate position indicated by the yellow region) in a normal elongation mode, the presence of nucleosomes causes long pauses (middle example) and stalled Pol II (right example).<sup>258</sup> Adapted from ref 258 with permission from Elsevier, copyright 2012.

decreased with increasing ionic strength, weakening histone–DNA interactions. For high ionic strength, the frequency of polymerase bypass was sufficiently high that the kinetics of bypass could be explored. Interestingly, pauses and backtracks occurring during the nucleosomal encounter were most pronounced in the first half of the nucleosome, and a Brownian

ratchet model was introduced to explain the observed pausing behavior. In this model, the polymerase uses local thermal unwrapping of the nucleosome to proceed forward, rather than actively removing DNA from the nucleosome.

A more detailed understanding of the location of polymerase pauses along the nucleosomal DNA was obtained in experiments performed by Michelle Wang and co-workers using a different experimental geometry, in which optical tweezers were used to mechanically unzip DNA.<sup>259</sup> The position of a bacterial RNAP on the DNA was inferred by a distinct pattern in the force–distance curve. In the experiments, transcription was initiated at a promoter, and the polymerase was stalled after a certain time delay. Subsequently, bound histone proteins were removed using heparin, and the position of the polymerase was mapped by mechanical unzipping of the DNA. A periodicity of 10 bp in the pausing location of the polymerase was reported, consistent with previous bulk transcription experiments using gel electrophoresis.

A recent single-molecule study by the Bustamante lab provided a deeper insight into the nature of the nucleosomal barrier.<sup>258</sup> The authors aimed at identifying the nucleosomal elements responsible for the observed pausing and backtracking of the polymerase by analyzing the nucleosomal bypass efficiency of Pol II and the duration of transcriptional pausing for four different nucleosomal constructs. In the first experiment, the importance of direct interactions of core histones with the nucleosomal DNA was tested by introducing two point mutations into the histone core, Sin H4 (H4 R45A) and Sin H3 (H3 T118A), whose effect on transcription through nucleosomes had previously been characterized in biochemical experiments.<sup>255</sup> In the single-molecule experiments, both histone mutations showed dramatic effects on Pol II transcription through the nucleosome: The nucleosomal bypass efficiency, the bypass speed, as well as the observed pause duration and frequency were all significantly different from those observed on unmodified nucleosomes and resembled the kinetics observed for transcription on bare DNA. Thus, mutations at these points dramatically weaken the nucleosomal barrier. Interestingly, a much smaller effect was observed if nucleosomes were used containing histones that fully lack their tails or histones with lysines that are usually subject to acetylation replaced by glutamines (effectively creating acetylated histones). Both of these histone modifications also increased the nucleosomal bypass efficiency, the bypass velocity, as well as decreased the observed mean pause duration during bypass, however to a much smaller extent than the Sin mutants. Interestingly, detailed analysis of the positions, at which most pauses were observed, yielded additional information about the nucleosomal barrier. While changes in the histone tails only altered the pause distribution at the entry side of the nucleosomes, the Sin mutants also reduced the pause density at the center of the nucleosome. One surprising outcome of this study is the finding that, despite their large mass, histone tails contribute only very little to the overall stability of the nucleosomes and thus to the nucleosomal barrier. This suggests that their role is rather to act as a binding platform for other proteins, such as ATP-dependent chromatin remodellers, which ultimately determines the fate of the nucleosome.

While the described optical tweezers experiments provide detailed insights into the nature of the nucleosomal barrier, they are not able to describe conformational changes the nucleosome undergoes during polymerase bypass. It is

commonly believed that one of the mechanisms of polymerase bypass involves the formation of a DNA loop, to which histones are transiently transferred. However, loop formation is most likely prevented in the optical tweezers experiments, where force acts on the DNA. Thus, alternative single-molecule techniques are required to be able to explore nucleosome structure during and after the bypass by the polymerase.

Recent AFM experiments provide a first glimpse at the nature of the nucleosome–Pol II complex during bypass.<sup>260</sup> In these experiments, Pol II and nucleosomes were assembled onto a single DNA molecule, and stalled (no nucleotides) or chased complexes were imaged in air, immobilized on a mica surface (Figure 9). Because transcription was not triggered and different polymerases translocate at different velocities, the resulting AFM images showed a mixture of complexes with the RNA polymerase upstream of the nucleosome, at the site of the nucleosome, or downstream of the nucleosome. Evidence for DNA looping during polymerase bypass comes from a quantification of the length of DNA flanking the protein complex (Figure 9e,f).

The single-molecule studies described in this section have drastically advanced our understanding of transcription in the context of chromatin. In the future, one could imagine to either monitor transcription through nucleosomes in real time using a high-speed AFM, following the pioneering work by Ando and co-workers on other motor proteins,<sup>151–153</sup> or report on structural changes of the nucleosome during polymerase bypass by means of smFRET experiments. The ultimate goal would be to combine experiments of transcription in the presence of nucleosomes with experiments of ATP-dependent nucleosome remodeling, because in the natural environment of the cell, part of the nucleosomal barrier might be lifted by the remodeling machinery.

## 5. TRANSCRIPTION INITIATION

Structural studies of transcription initiation complexes have tremendously advanced our understanding of this complex process;<sup>12,261–266</sup> however, many aspects of transcription initiation remain elusive. One of the key remaining questions is how conformational changes of the polymerase in the open as well as the initially transcribing complex lead to a controlled transition from transcription initiation to elongation. In particular, an explanation had to be found for the observation of footprinting studies that the amount of DNA protected by the polymerase increases during transcription initiation. On the basis of biochemical observations, three different mechanical models were proposed: (i) transient back and forth movement of the polymerase, (ii) inchworming of the polymerase, or (iii) uptake of additional downstream DNA into the initiation complex (scrunching model) (Figure 10a). These models were elegantly tested in two different single-molecule experiments.

First, Shimon Weiss and co-workers used smFRET measurements to measure distance changes within the bacterial RNAP initiation complex during transcription initiation.<sup>131</sup> As an example, they compared the distance between positions DNA–15 and DNA+15 in the open complex (RP<sub>O</sub>) as well as in initially transcribing complexes (RP<sub>itc</sub>) (Figure 10b). Their smFRET histograms show a clear change in the mean FRET efficiency as well as in the general shape of the histogram, indicating a scrunching of the DNA. Additional evidence for the scrunching model came from measurements of smFRET efficiencies between various positions on initiation factor  $\sigma^{70}$  and positions on the downstream or upstream DNA. All results

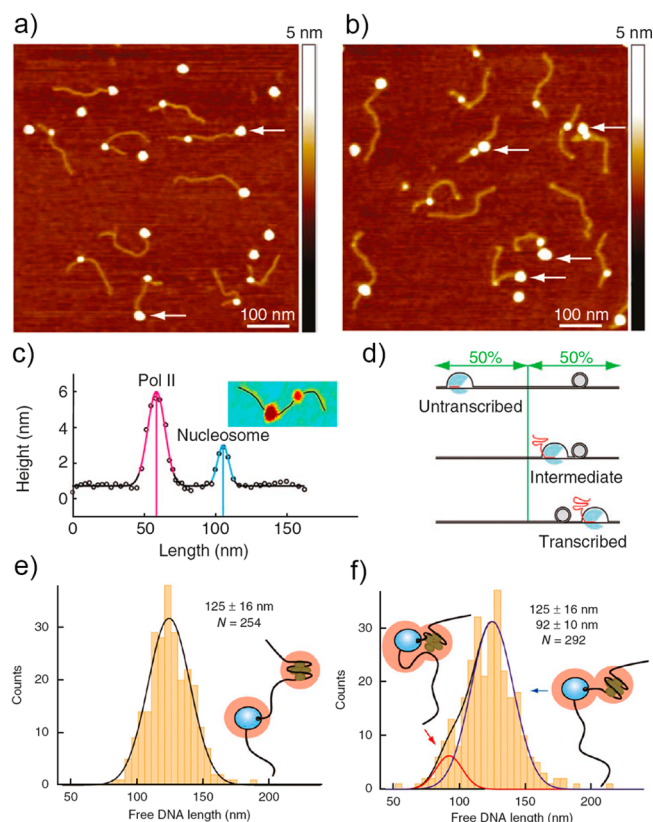


**Figure 9.** AFM imaging of transcription through nucleosomes. (a) AFM image of stalled polymerases on DNA molecules containing mononucleosomes. Complexes were assembled but not chased in solution, cross-linked, attached to mica, and imaged in air. Note that not all DNA molecules contain both polymerase and nucleosome. (b) AFM images of the same sample as in (a) after chasing with all four nucleotides. Some polymerases have bypassed the nucleosomes. (c) Exemplary height profile showing the difference in the height of the polymerase and the nucleosome. The difference in height allows for a clear distinction in the experiment. Note that due to the imaging in air (and the high forces during imaging), the observed height is lower than the expected height. (d) Schematic explaining the design of the DNA construct and data analysis. Before chasing, the polymerase sits on one-half of the DNA, while the nucleosome sits on the other half of the DNA downstream from the polymerase (at about 75% of the contour length). After chasing, one can see if the polymerase was active, that is, has left the first half of the DNA, was stalled, that is, sits in front or at the position of the nucleosome, or was able to bypass the nucleosome, that is, sits on the short end of the DNA with the nucleosome at an upstream position. (e) Histogram of observed free DNA length for the situation where the polymerase has started transcription, but has not yet reached the nucleosome. The histogram shows a single peak centered at a length of 125 nm. (f) Histogram of observed free DNA length for situations where the polymerase and the nucleosome cannot be separated spatially. Now, the histogram has to be fitted by a double distribution, one with the length identical to that in (e) and one with a reduced length of free DNA of 92 nm. The presence of this second population indicates that during the bypass a loop of DNA is captured between the polymerase and nucleosomes. It had been speculated for a long time that the presence of DNA loops could help in transferring the DNA from a position downstream of the polymerase to an upstream position.<sup>260</sup> Adapted from ref 260 with permission from Nature Publishing Group, copyright 2011.

showed the same effects: The relative position of the upstream DNA with respect to the position on  $\sigma^{70}$  remained unchanged during transcription initiation, while all positions on the

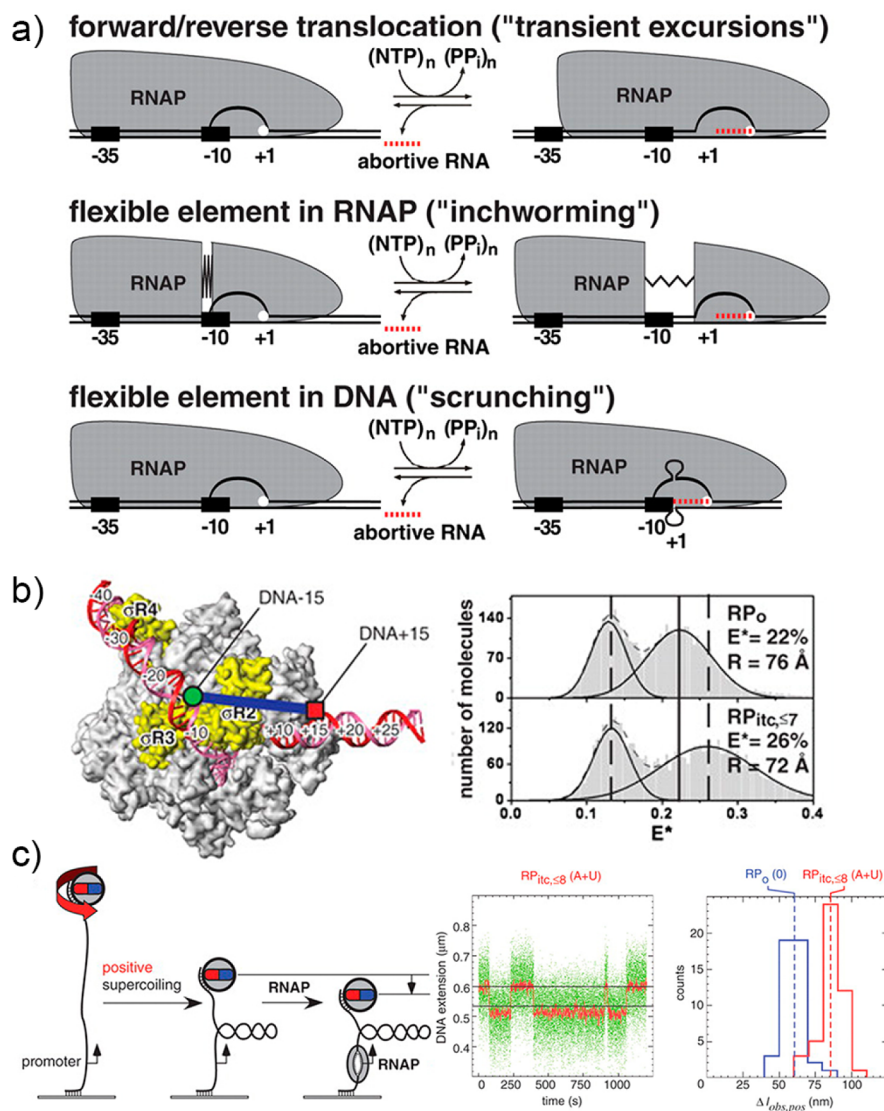


**Figure 10.** Scrunching of DNA during transcription initiation. (a) Different models for transcription initiation explaining the observed expanded footprint of the polymerase.<sup>131</sup> (b) Scrunching is observed in smFRET experiments. Labeling of the DNA at positions  $-15$  and  $+15$  with a donor and acceptor dye, respectively, enables visualization of the movement during transcription initiation. The observed smFRET histograms show two peaks, one from the free DNA and one from the DNA bound to the polymerase in the  $RP_0$  or  $RP_{itc}$  complex. The observed mean smFRET efficiencies shift to higher values as the DNA is pushed into the initially transcribing complex.<sup>131</sup> (c) DNA scrunching observed with magnetic tweezers. A single DNA molecule containing the promoter sequence is stretched and then positively supercoiled using a rotating magnetic bead. As the polymerase binds to the bead and starts scrunching, it introduces additional positive supercoils. As a result, the bead will be pulled closer to the surface. The data show a measured time trajectory as well as the distribution of distances. By using only a limited set of nucleotides, it was possible to determine after how many steps a positive supercoil is added. For short transcripts of one or two nucleotides, there was no change in DNA length. However, if production of up to 8nt long RNA was allowed, the formation of positive supercoils could be observed.<sup>269</sup> (a), (b) Adapted from ref 131 with permission from The American Association For The Advancement Of Science, copyright 2006. (c) Adapted from ref 269 with permission from The American Association For The Advancement Of Science, copyright 2006.

downstream DNA moved toward the polymerase. This result manifests DNA scrunching. Similarly, DNA scrunching during transcription initiation was observed for the single subunit RNA polymerase from T7.<sup>267,268</sup> Interestingly, DNA scrunching as well as rotations during early RNA synthesis and not structural changes within the T7 RNA polymerases were rate limiting for the transition from initiation to elongation, suggesting that these processes are key regulatory steps of transcription.

A completely different approach to test the scrunching model for RNAP transcription initiation was used by Strick and co-workers,<sup>269</sup> who performed single-molecule extension and twisting experiments using magnetic tweezers. In magnetic

tweezers, a single DNA molecule is stretched by application of a magnetic force to the molecule.<sup>123,124,270</sup> To this end, one end of the DNA molecule is attached to a glass slide, whereas the other end is attached to a superparamagnetic bead. The bead is then lifted upward by moving a magnet away from the surface (Figure 10c). By rotating the magnet, one can rotate the bead and in this way apply twist to the DNA molecule if the attachment assures that the molecule is torsionally constraint. Applying twist in one or the other directions leads to positive or negative supercoiling of the DNA. Because the RNA polymerase unwinds DNA while transcribing, movement of the polymerase can be visualized by a change in the supercoiling

density, which in turn manifests itself in a change of observed DNA length (Figure 10c).<sup>271</sup> From the three different mechanical models of transcription initiation presented above, only in the DNA scrunching model the number of supercoils in the DNA is expected to change by an initiating enzyme. Therefore, measuring the number of supercoils during transcription initiation allows for directly testing the scrunching model. In the experiments, the production of truncated transcripts, that is, abortive initiation, was induced by providing only a limited set of nucleotides to the polymerase. For short transcripts of one or two nucleotides, no change in DNA length was noted. However, if production of up to 8nt long RNA was allowed, formation of positive supercoils could be observed in accordance with the DNA scrunching model.

Recent smFRET-based studies have shed light on the dynamics of the bacterial RNAP during transcription initiation. Kapanidis and co-workers showed that the open promoter complex undergoes dynamic conformational changes on the millisecond time scale.<sup>272</sup> They argue that this flexibility is connected to the variability of start site selection of RNAP and that factors such as DNA sequence, availability of nucleotides, or the presence of regulating factors could alter start site selection. Moreover, Ebright and co-workers recently investigated the closing and opening of the RNAP clamp during transcription initiation using smFRET (Figure 11).<sup>273</sup> They

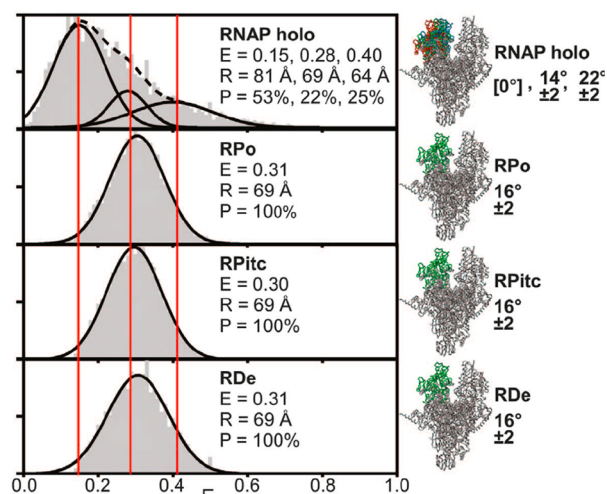


**Figure 11.** Rearrangement of the RNAP clamp during transcription initiation. The conformation of the RNAP clamp was investigated using smFRET. The dye molecules were attached at the tip of the clamp (donor) and at the tip of the  $\beta$  pincer. The observed smFRET distribution of the free polymerase bound to  $\sigma^{70}$  (RNAP holo) has to be fitted with at least three Gaussian distribution, indicating that at least three states are observed. In the open complex (RPo), the initially transcribing complex (RPitc), as well as in the elongating complex (RDe), only a single distribution is needed to fit the data. The determined mean smFRET distribution for RPo, RPitc, and RDe is always  $E = 0.3$ , which is close to the mean efficiency of the middle peak of the RNAP holo ( $E = 0.28$ ). However, this middle peak is only the minor contribution for RNAP holo. The histogram is dominated by a low smFRET of  $E = 0.15$ , which accounts for more than 50% of the data. Additionally, 25% of the data are fitted by a distribution centered at  $E = 0.4$ , indicating that there is a third more collapsed state present, or maybe more probable multiple states or conformational heterogeneity, because this peak is extremely broad.<sup>273</sup> Adapted from ref 273 with permission from The American Association For The Advancement Of Science, copyright 2012.

found that the holoenzyme and the core polymerase showed an open conformation in equilibrium with several closed states, whereas the clamp in the open complex, the initially transcribing complex, as well as the elongation complex existed in a closed conformation. Comparison of the smFRET data with structural and molecular dynamics data indicated that the closed and the open states observed by smFRET are in good agreement with the states previously reported in X-ray structures. In summary, the study shows that loading of the DNA into the active center cleft of the polymerase requires the clamp to be in the open state. Upon loading of the DNA, the clamp appears to be locked in the closed conformation, thus clamping down on the DNA and ensuring processivity of the enzyme.

While the bacterial RNAP is dependent only on one initiation factor, the eukaryotic enzyme requires the interplay of a large set of transcription factors to initiate transcription, most importantly general transcription factors TFIIA, -B, -D, -E, -F, and -H. These factors assemble at the promoter and recruit Pol II to form the preinitiation complex. The large size, heterogeneous composition, and dynamic nature of eukaryotic initiation complexes have made studies of Pol II transcription initiation difficult, especially using standard structural methods such as X-ray crystallography.

First direct insight into transcription initiation comes from single-molecule fluorescence experiments of the Tijan and Chu laboratories.<sup>274</sup> Using purified human Pol II as well as purified general transcription factors, they were able to develop a video microscopy assay for following various steps in promoter directed transcription initiation of Pol II. The authors were able to detect transcription events at the single-molecule level and could show that transcription is enhanced by the human regulator Sp1.

A recent study by Treutlein et al. used smFRET in combination with global NPS analysis<sup>110</sup> to determine the molecular architecture of a minimal Pol II open promoter complex (OC).<sup>275</sup> The investigated minimal OCs were assembled from promoter DNA including a TATA box and an 11-nucleotide mismatched region around the transcription start site, Pol II, TBP, and general transcription factors IIB and IIF. The authors measured smFRET efficiencies between antenna dye molecules attached to the upstream nontemplate DNA, the TATA box, TBP, and TFIIB, and several satellite dye molecules attached to positions on the template DNA and Pol II Rpb4/7. They then used global NPS analysis to obtain the position of the upstream DNA including the TATA region, TBP, and TFIIB relative to Pol II. An architecture of the OC was revealed, in which TATA–DNA and TBP reside above the Pol II cleft between clamp and protrusion domains. TFIIB was displaced from the Pol II wall, where it is located in the closed promoter complex. Most interestingly, time trajectories of smFRET measurements between the TBP–TATA subcomplex and the downstream DNA showed dynamics (Figure 12), which were assigned to the movement of downstream DNA into and out of the Pol II cleft. This dynamic loading and unloading process happened at a time scale of seconds and hence represents a major kinetic trap in the assembly process. This intrinsic flexibility also explains why minimal Pol II OCs could not be trapped crystallographically.

NPS experiments on Pol II transcription initiation have the difficulty that currently available labeling sites are limited to Rpb4/7, the nucleic acids, or to other transcription initiation factors such as TFIIB and TBP. Here, the archaeal RNA

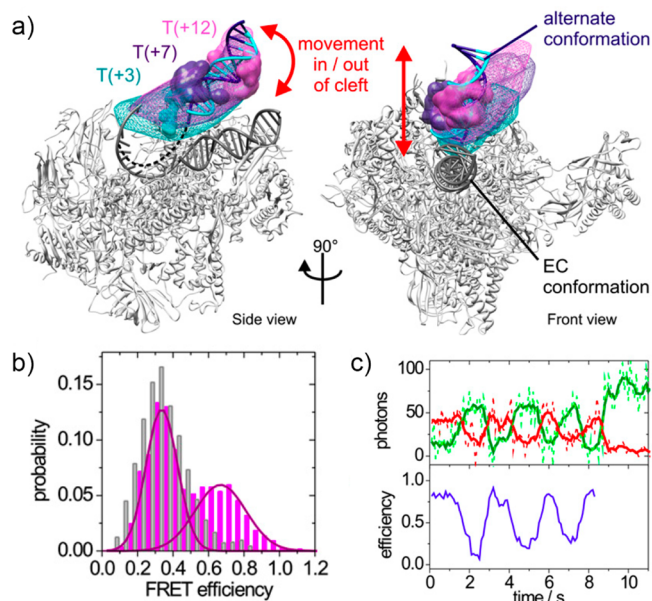


**Figure 12.** Dynamics of downstream DNA during transcription initiation. (a) The downstream DNA within open promoter complexes was observed in smFRET experiments to capture two different conformations: the EC conformation in the cleft (gray) as well as an alternate conformation outside of the cleft as revealed by global NPS analysis. The position probability densities resulting from global NPS analysis of the antennas attached to the downstream DNA are shown as meshed credible volumes contoured at 68% probability relative to the Pol II EC.<sup>5</sup> (b) smFRET measurements for satellite positions on the downstream DNA resulted in FRET efficiency histograms with two populations, indicating the alternate conformation of the downstream DNA. (c) Downstream DNA in Pol II open complexes switches dynamically between positions inside and outside of the cleft. Example of directly observed dynamic transitions between low- and high-FRET state. Time trace of fluorescence intensities (dashed lines, raw data, and solid lines, 5 point moving average) for donor NT-DNA(−30)-Tamra (green) and acceptor T-DNA(+3)-Alexa647 (red) are shown together with the computed FRET efficiency (blue). Adapted from Treutlein et al.<sup>275</sup>

polymerase provides an interesting alternative. The RNA polymerase from archaea is structurally highly homologous to both Pol I and Pol II,<sup>276</sup> and the mechanistic studies on the *M. janaschii* enzyme have several experimental advantages. First, an *in vitro* reconstitution assay of the complete 12 subunit enzyme has been developed, yielding the possibility for straightforward fluorescent labeling at any desired position on the enzyme,<sup>277</sup> thus opening the way for structure function analysis of the enzyme using single-molecule fluorescence methodologies. Second, promoter-dependent transcription initiation can be established comparatively simply, by using complexes of polymerase, TBP, TFB, and optionally TFE as well as promoter DNA.<sup>278</sup> Third, the structure and function of several of the important basal transcription factors is believed to be almost identical from archaea to eukaryotes. In first NPS experiments on this system, the position of the winged helix domain as well as that of the zinc ribbon domain of TFE in the transcription initiation complex were determined (Figure 13a).<sup>215</sup> Interestingly, the determined position of the winged helix domain, which was shortly thereafter verified by chemical cross-linking,<sup>279</sup> overlapped with the previously determined binding site of Spt4/5 on the polymerase.<sup>280</sup> This suggests that TFE and Spt4/5 could kinetically compete for the same interaction

site and binding of one factor could displace the other. Using EMSA, it has been shown that TFE and Spt4/5 are indeed competing for binding to the polymerase *in vitro* (Figure 13b). Yet, the roles of the two factors are remarkably different. In the transcription initiation complex, binding of Spt4/5 reduces the observed transcription (Figure 13c), while TFE stimulates transcription. However, the negative effect of Spt4/5 can be overcome by TFE, presumably outcompeting Spt4/5 for the binding site on the polymerase in the transcription initiation complex. In the elongation complex, TFE has no effect on transcription, while Spt4/5 stimulates transcription (Figure 13d). Here, Spt4/5 outcompetes TFE, because the stimulation is not reduced by the presence of TFE.

This example shows how changes in the affinity of the transcription machinery for different transcription factors can both regulate and control their relative efficiencies of binding, as well as affect the fidelity of transcription. It will be important to see in future experiments whether this is a common mechanism that is exploited in different variations throughout transcriptional regulation in prokaryotes and eukaryotes. Besides the observed specific binding site on the surface of the polymerase, another likely candidate for a binding platform is the C-terminal domain of Pol II. Post-translational modifications of the heptad repeat of the CTD act as modulators for transcription factor affinity to the polymerase, thus adding another level of complexity to the delicate control of transcription in eukaryotes.<sup>281</sup>

Besides the dynamics of the transcription initiation complexes, another important aspect for understanding this process is the question of how the polymerase finds the promoter. Recently, elegant single-molecule experiments by Greene and co-workers using DNA curtains,<sup>282</sup> to obtain data in a fast and massively parallel assay, have yielded insight into the search mechanism.<sup>283</sup> They were able to show that *in vitro*, the promoter search by RNAP is dominated by three-dimensional diffusion not only for distant searches, but also for submicroscopic length-scales. This search strategy is successful also in the very crowded cellular environment, where other proteins bound to DNA would provide obstacles to an RNAP molecule diffusing one-dimensionally on the DNA.

One of the most studied aspects of transcription regulation is the interaction of the polymerase with proteins that enhance or repress transcription. One of the most prominent examples is that of the lac operon, where the lac repressor is known to repress transcription by competing with the polymerase in promoter binding. Interestingly, recent single-molecule experiments by the Gelles lab using single-molecule fluorescence colocalization and photobleaching of a dye labeled RNAP have shown that the polymerase can bind in a stable fashion to more than one site on a promoter DNA.<sup>284</sup> The lac repressor prevents binding to one of those sites, thus preventing the formation of transcriptionally competent complexes, but does not impede binding to the secondary site. Using the same single-molecule fluorescence colocalization technique, also the kinetic mechanism of bacterial transcription initiation at  $\sigma^{54}$  promoters has been investigated.<sup>285</sup> The single-molecule experiments can reveal interesting kinetic intermediates of the closed complex of  $\sigma^{54}$  with the slowest step being the transition of the second closed complex state to the open complex. The transition to the open complex state also marks the commitment step during  $\sigma^{54}$  transcription initiation.

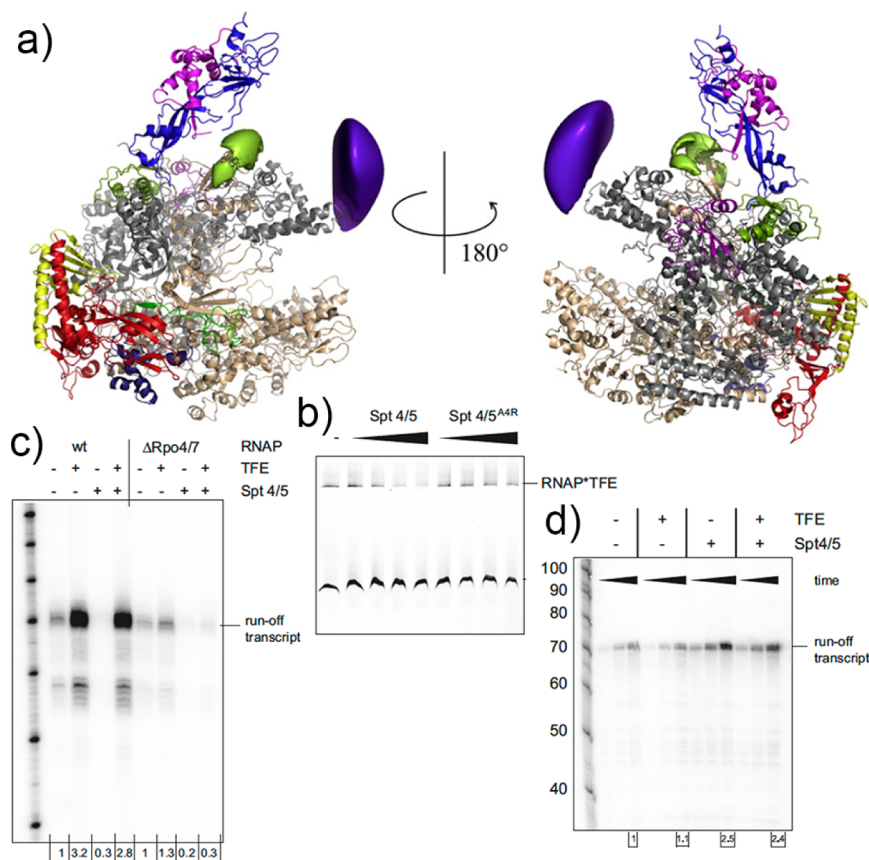


**Figure 13.** Competition of transcription initiation factor TFE and transcription elongation factor Spt4/5 for the same binding site on the polymerase. (a) NPS localization of a dye molecule attached to the zinc ribbon domain (green) and another dye molecule attached to the winged helix domain (purple) of TFE with respect to the archaeal RNA polymerase. (b) Competition of binding of TFE and Spt4/5 to the polymerase studied by EMSA. (c) Binding of Spt4/5 to PIC abolishes transcription activity, which can be rescued by TFE. (d) In the elongation complex, Spt4/5 increases the transcription activity whereas TFE does not.<sup>215</sup> Adapted from ref 215 with permission from Elsevier, copyright 2011.

## 6. TRANSCRIPTION TERMINATION

Single-molecule studies of transcription termination have so far only focused on the bacterial RNA polymerase. In prokaryotes, specific sequences called intrinsic terminators are known to cause transcription termination. The sequence motifs of such terminators consist of a region that allows for the formation of an RNA hairpin, followed by an A-rich region in the DNA template resulting in a slippery U-tract. In an elegant study, Block and co-workers used optical tweezers to measure the termination efficiency of three different terminator sequences by applying both opposing and assisting force (Figure 14).<sup>286</sup> The termination efficiency was independent of the load on the DNA; however, the kinetics of termination were altered, in some instances leading to a stalled polymerase. Interestingly, in contrast to polymerase pausing during elongation, this state, termed a terminal dwell, was not followed by further elongation but by a release of the DNA template, thus constituting an intermediate step during the termination process.

These experiments illustrate one of the main strengths of optical tweezers experiments for the investigation of enzymatic reactions. By investigating how the reaction is altered as a function of force, one is able to reveal the underlying energetic landscape, thus getting direct insight into the molecular mechanism of a certain reaction.<sup>287,288</sup> In particular, steps along the enzymatic cycle that involve a translocation along the mechanical reaction coordinate are prone to be highly force sensitive.

Maybe the most important clue toward understanding the mechanism of sequence dependent transcription termination in bacteria came from experiments where force was applied to the nascent RNA transcript.<sup>289</sup> To exert force on the nascent RNA, the polymerase is bound to a bead held in an optical trap, and a single-stranded DNA sequence complementary to the 5' end of the nascent RNA is used to form a DNA–RNA hybrid and to attach the nascent RNA to another bead held in the second trap. In such an experiment, the formation of hairpins can be prevented. Detailed knowledge of RNA hairpin stability existed from controlled unfolding experiments using optical tweezers.<sup>290,291</sup> To separate the effect of the U-tract region from that of the RNA hairpin, experiments were done with termination sequences containing only the U-tract, or both the U-tract as well as the terminator hairpin. For all investigated terminators, no difference in termination efficiencies could be observed for forces above the hairpin unfolding forces ( $\sim 18$  pN) (Figure 14c). For forces below the hairpin unfolding force, transcript release increased with force. Interestingly, force does not only influence formation of the terminator hairpin, but also that of other secondary structures in the nascent RNA. The experiments led to a quantitative model for the sequence-dependent intrinsic termination of RNAP. In this model, there are two important energetic terms, the free energy of the DNA–RNA hybrid as well as the free energy of the hairpin. Moreover, two distances are important: the distance  $d_{\text{hybrid}}$ , which is the amount of shearing of the RNA that leads to a release of the

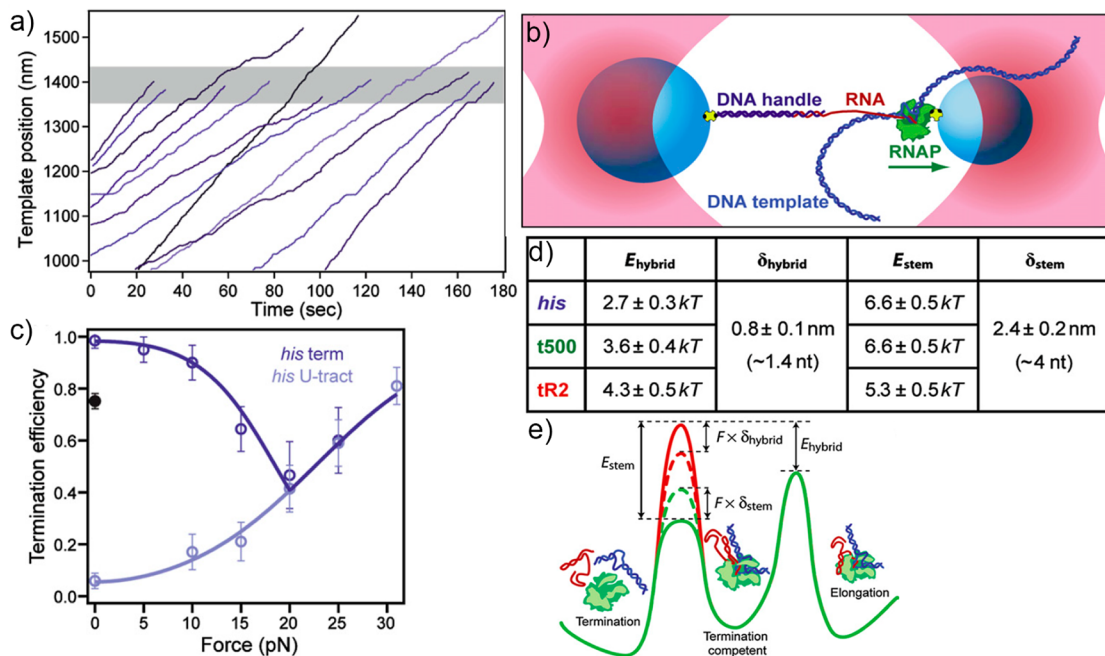


**Figure 14.** Transcription termination. (a) Exemplary single-molecule transcription events showing preferred termination at the location of the his-terminator sequence (gray area). Experiments were performed at 18 pN of assisting force. (b) Experimental geometry for measurements with force applied to the nascent RNA. A double-stranded DNA handle is used together with a DNA–RNA hybrid to pull on the elongated strand. The polymerase is attached to a second bead in the dumbbell tweezers design. (c) Experimentally determined termination efficiency as a function of applied force for the *his* terminator sequence, as well as for the *his* U-tract, that is, where the terminator hairpin has been removed. The zero force data point is obtained from bulk gel-based assays, and the black data point is also from bulk assays, however, in the presence of complementary oligos to prevent the formation of secondary structure. (d) Overview of the parameters describing the modeled free energy landscape, which is illustrated in (e). Adapted from ref 286 with permission Elsevier, copyright 2008.

transcript, and  $d_{\text{stem}}$ , which corresponds to the distance necessary for formation of a stable RNA termination hairpin.

It would be exciting if similar experiments could also be performed for factor dependent termination. For example, in bacteria, Rho helicase is thought to use an allosteric mechanism to facilitate termination.<sup>292</sup> In eukaryotes, mRNA transcriptional termination is more complex and involves polyadenylation followed by digestion of the 3' end of the RNA by an exonuclease in a “torpedo-like” fashion.<sup>293–295</sup> Recent work has even revealed that termination of cryptic transcripts and short RNAs is tightly connected to RNA 3'-end processing adding another realm for future mechanistic studies of termination using single-molecule methods.<sup>296–298</sup>

## 7. SINGLE-MOLECULE STUDIES OF TRANSCRIPTION IN SINGLE CELLS

Ultimately, the action of single RNA polymerases has to be understood in the complex environment of a living cell. Single-molecule *in vivo* studies of transcription using fluorescence microscopy have provided invaluable new insights into the dynamics and regulation of transcription in single cells.<sup>18,20,299</sup> One of the most surprising results was the observation that transcriptional activity, instead of being tightly regulated and deterministic as previously thought, actually varies from cell to cell and exhibits large temporal fluctuations within a single cell. The fluctuations were attributed to random bursts of transcriptional activity, in which many mRNA molecules are transcribed within a short time period followed by periods without active transcription.<sup>300,301</sup>

Transcriptional bursting was first detected by Golding et al. in single bacterial cells (Figure 15a).<sup>164</sup> Using the MS2-GFP

technique (see section 2.4), the authors followed the synthesis of an exogenous mRNA target consisting of the coding sequence of a red fluorescent protein (mRFP) and a tandem array of 96 MS2 binding sites and directly observed transcriptional bursts in the time-series data. Because the target mRNA was translated into a fluorescent protein, the authors were also able to compare mRNA and protein levels in single cells and found them to be proportional. Since this initial work in bacteria, transcriptional bursting has been observed in a variety of systems ranging from slime mold to mammalian cells,<sup>159,172,302,303</sup> and therefore appears to be a ubiquitous mode of transcription.

The Singer lab was the first to detect the bursting behavior of RNA polymerase II transcription in eukaryotes.<sup>172</sup> An endogenous developmental gene was investigated in *Dictyostelium* using the MS2-FP technique, and discrete pulses of transcriptional activity were observed. Surprisingly, the length and height of pulses were consistent throughout development; however, the fraction of single cells showing active transcription varied over the course of development. Another finding of this study was the presence of transcriptional memory: cells were more likely to retranscribe a gene that had been previously active than to initiate transcription *de novo*. The first demonstration of transcriptional bursting of RNA polymerase II in mammalian cells comes from a study by Raj et al.,<sup>159</sup> in which a reporter gene was stably integrated into the genome of Chinese hamster ovary cells and mRNA was detected on the single-molecule level by means of mRNA-FISH (Figure 15b). The authors showed that transcriptional bursts were intrinsically random and not due to global, extrinsic factors such as levels of transcription activators; however, genes within a wider

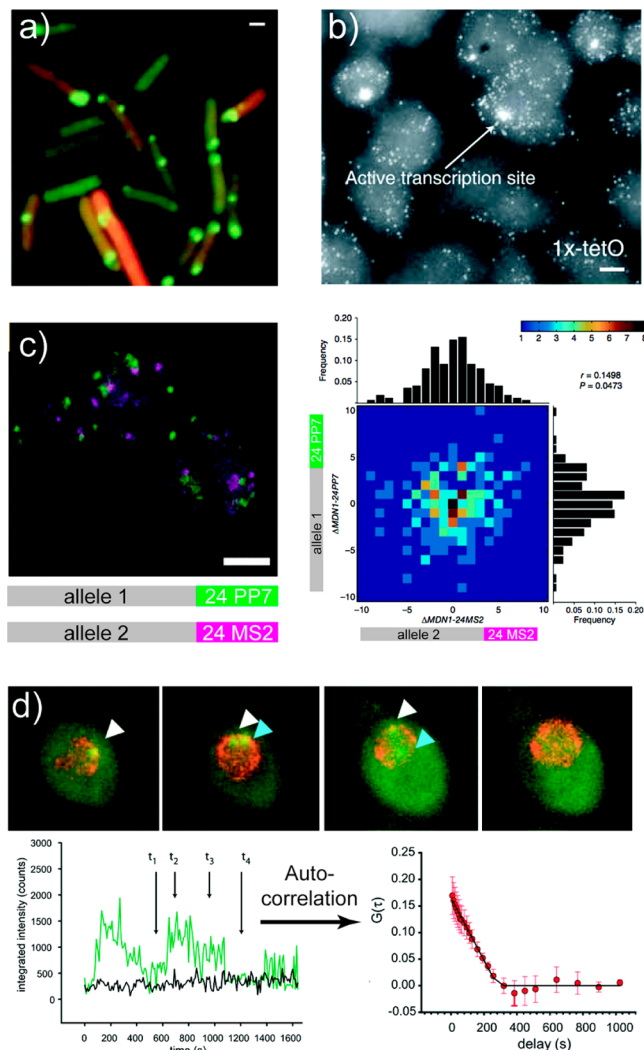


**Figure 15.** Single-molecule studies of transcription in single living cells. (a) First detection of transcriptional bursting by Golding et al. in single *Escherichia coli*.<sup>164</sup> Single RNA molecules encoding the red fluorescent protein were fluorescently labeled using the MS2-GFP and a tandem array of 96 MS2 binding sites (green, mRNA; red, red fluorescent protein). (b) First observation of stochastic mRNA synthesis in mammalian cells by Raj et al. using the RNA-FISH approach.<sup>159</sup> Representative field of cells from a Chinese hamster ovary cell line. Sites of active transcription are detected as bright spots. (c) Single-molecule analysis of gene expression of the two alleles of a gene using two-color RNA labeling in living yeast cells.<sup>309</sup> A cassette of 24 PP7 (green) or MS2 (magenta) binding sites was inserted into the 3' UTR of either two alleles of the yeast MDN1 gene, respectively. The two alleles showed independent transcriptional fluctuations as no correlation was observed (right panel). (d) Top: Real-time observation of transcription of an endogenous gene in a single living yeast cell. Sites of active transcription are marked by arrows. Images were recorded after 0, 2, 22, and 28 min. Bottom: Fluorescence intensity time trajectories of the transcription site reveal multiple Pol II enzymes transcribing the gene at the same time. At time  $t_1$  a single Pol II is loaded on the gene, whereas at time  $t_2$  multiple Pol IIs are transcribing the gene. At  $t_3$  the first RNAPII has terminated, and at  $t_4$  all Pol IIs have left the gene. Fluctuation analysis of fluorescence time trajectories reveals the rate of transcription elongation. (a) Adapted from ref 164 with permission from Elsevier, copyright 2005. (b) Adapted from Raj et al.<sup>159</sup> (c) Adapted from ref 309 with permission from Nature Publishing Group, copyright 2012. (d) Adapted from ref 162 with permission from The American Association For The Advancement Of Science, copyright 2011.

genomic locus appeared to be activated in a correlated way. Transcriptional bursting in eukaryotes is not limited to genes transcribed by Pol II. An mRNA-FISH study by the van Oudenaarden lab showed that transcription of rRNA by Pol I occurred in bursts as well.<sup>304</sup>

Two recent studies in bacteria and *Dictyostelium* have provided further insights into the characteristics of transcriptional bursting. So et al. showed that in single bacterial cells, the extent of transcriptional bursting showed direct correlation to its average expression level.<sup>161</sup> Moreover, work in *Dictyostelium* by the Chubb lab demonstrated that the frequency of transcriptional bursting is not only variable over the population of cells, but is also a heritable trait. The persistence of transcriptional fluctuations from one generation to the next was shown to be dependent on histone H3K4 methylation.<sup>305</sup>

Even though bursting has been observed in many systems, other transcription dynamics have been observed as well. In yeast, single mRNA counting by means of mRNA-FISH revealed that genes, especially housekeeping genes, exhibit a constitutive mode of transcription with unexpectedly small variations. This is a consequence of transcription events occurring randomly over time and with a constant probability.<sup>162,306</sup>

An interesting question concerning transcriptional dynamics in single cells is whether functionally related genes or even the two alleles of the same gene are transcribed in a correlated way. Gandhi et al. addressed this question by simultaneously counting individual mRNAs of functionally related and unrelated genes in single yeast cells using mRNA-FISH.<sup>307</sup> They found that transcript levels of temporally induced genes are highly correlated within single cells; however, constitutive genes encoding essential subunits of protein complexes such as general transcription factor (TF) IID or RNA polymerase II are not correlated any more than functionally unrelated genes. In addition, the authors explored transcription of the two alleles of the same gene by introducing a cassette of RNA hairpins from bacteriophage PP7 into the 3' UTR of only one of the alleles and targeting it with separate FISH probes. Only a weak correlation between the mRNA levels of the two alleles was observed, a fact that was confirmed by a more recent work of the Singer laboratory, in which the two alleles of the same gene were labeled with different colors using PP7-GFP as well as MS2-mCherry in diploid yeast cells (Figure 15c).<sup>158</sup>

Several recent studies took a more integrative approach to investigate transcription in single living cells. Darzaq et al. used a locus specific reporter system in single human cells in combination with FRAP measurements to quantify both RNA polymerase II and mRNA kinetics in vivo with a high temporal resolution.<sup>170</sup> Single mRNA molecules were detected using MS2-FP or mRNA-FISH labeling, and RNA polymerase II was visualized through fusion to the YFP. Moreover, immunostaining of fixed cells was used to detect the phosphorylation state of Pol II. Pol II elongated at 4.3 kilobases per minute and entered a paused state for unexpectedly long times. Moreover, transcription onset was very inefficient, with only 1% of polymerase–gene interactions leading to completion of a mRNA.

Another interesting question is whether cotranscriptional RNA processing such as splicing modulates the rate of transcription. The correlation between transcription elongation and cotranscriptional splicing was explored in a recent study of the Shav-Tal laboratory.<sup>180</sup> In a human cell line,  $\beta$ -globin was studied as a model gene, and different constructs were designed

that either contained varying numbers of intron/exons and were therefore subject to cotranscriptional splicing or did not contain any intron and were therefore not expected to recruit the spliceosome. Single nascent mRNA molecules were detected via MS2-FP labeling, and individual RNA subunits of the spliceosome were labeled by means of RNA-FISH probes. Spliceosomes were observed to accumulate on intron-containing genes with the number of spliceosomes increasing with the number of introns. Moreover, kinetic measurements of the Pol II elongation rate showed that transcription elongation kinetics proceeded independent of the presence of cotranscriptional splicing at the  $\beta$ -globin gene. Another study that investigated transcriptionally coupled and uncoupled splicing used the molecular beacon approach to label the exon and intron region of synthesized mRNA with spectrally distinct fluorophores (Figure 5d).<sup>177</sup> A loss of colocalized emission from both fluorophores indicated a splicing event. Using this approach, the authors found that the normally tight coupling between transcription and splicing is broken in situations where the intron's polypyrimidine tract is sequestered within strong secondary structures.

The binding of upstream activators and transcription factors to the promoter region is essential for Pol II recruitment to the promoter and transcription initiation. However, the connection between upstream transcription activator and downstream transcriptional regulation is not well understood. Scientists in the McNally laboratory addressed this lack of knowledge using yeast as a model system.<sup>308</sup> FRAP and ChIP were used to measure the dwell time of the GFP labeled activator ACE1 on an endogenous tandem array, and the transcribed mRNA was detected by MS2-FP labeling. Both fast and slow cycling of the activator was observed simultaneously on the endogenous yeast promoter, and whereas fast cycling initiated transcription, slow cycling regulated the quantity of mRNA production.

The first direct measurement of transcription of single nascent mRNA molecules from an endogenous, cell-cycle regulated yeast gene was recently achieved by the Singer laboratory (Figure 15d).<sup>162</sup> Larson et al. introduced a cassette of PP7 bacteriophage coat protein binding sites into either the 3' or the 5' UTR of the endogenous gene of interest, such that binding of PP7-GFP fluorescently labeled the nascent RNA either right after initiation or shortly before termination of transcription. As a consequence, the 5' UTR construct enabled the authors to obtain time-lapse data for whole transcription cycles, whereas the 3' UTR construct was sensitive only to late events in the lifetime of a nascent RNA molecule (see section 2.4, Figure 5d). In addition, Larson et al. developed a novel, quantitative method of fluctuation analysis of fluorescently labeled mRNA to measure the kinetics of transcription initiation and the dynamics of elongation and termination. By combining the data from both gene constructs, it was possible to determine kinetic rates of initiation and elongation. The analysis revealed that different Pol II's acted in an uncorrelated manner on the investigated gene, and that elongation proceeded processively at a steady rate without being interrupted by major pausing of Pol II. Nevertheless, throughout the cell cycle the elongation rate varied 3-fold, and also initiation rates were observed to be cell-cycle dependent. Finally, Larson et al. correlated transcription of the mRNA with the diffusion and binding behavior of an upstream transcription factor measured by FCS. As a result, transcription initiation of the investigated gene was dependent

only on the success of the transcription factor in its search for its particular promoter binding site.

Single-molecule, single cell studies of transcription such as those presented in this section will pave the way to a more mechanistic understanding of the dynamics of transcription regulation in the complex cell environment.

## 8. OUTLOOK

Single-molecule methods have in the last two decades advanced from simple demonstration experiments to a level where quantitative mechanistic insight can be obtained. While initial experiments investigated rather simplistic scenarios, where a single enzyme moves along a single DNA molecule, lately, researchers are trying to add to the complexity of the situation, by including regulatory factors or by studying dynamic transient processes where the composition and architecture are changing rapidly. It is precisely these scenarios where single-molecule techniques are prone to have their highest impact. Investigating processes at the single-molecule level, or maybe one should better say at the single complex level, allows for the direct, real-time visualization and manipulation of crucial molecular steps within cells. Clearly, more research is needed for understanding the intricate interaction of transcription and other processes. First experiments in living cells or using higher order structures have already been performed and are laying out the path for future research. However, the field will only advance as fast as method development is advancing as well. For example, superfast AFM imaging, super-resolution optical microscopy, single particle tracking, smFRET experiments in living cells, and other techniques will be crucial, and their continued improvement is needed for future advances in the field of single-molecule studies of transcription.

## AUTHOR INFORMATION

### Corresponding Author

\*Phone: +49 731 50 23050. Fax: +49 731 50 23059. E-mail: jens.michaelis@uni-ulm.de.

### Notes

The authors declare no competing financial interest.

### Biographies



Jens Michaelis obtained his Ph.D. in physics in 2000 under the supervision of Prof. Vahid Sandoghdar and Prof. Jürgen Mlynek at the University of Konstanz. He then moved to Berkeley to the group of Prof. Carlos Bustamante to work on single-molecule biophysics of molecular motors. In 2003 he started his own independent group at the Department of Chemistry and Biochemistry at Munich University.

He was promoted to W1 professor in 2006 and W2 professor in 2008. Since 2011 he is a full professor and head of the Biophysics Institute at Ulm University. In his research he has applied novel single-molecule techniques to research in biophysics, in particular to the field of transcription, as well as in materials science. His work has appeared in journals such as *Nature*, *Cell*, *Molecular Cell*, *PNAS*, *Nature Methods*, *Nature Nanotechnology*, and *Nano Letters*. His research has been awarded the prestigious Nernst-Haber-Bodenstein Award as well as the ERC starting grant.



Barbara Treutlein received her Diploma in Chemistry from the University of Tübingen and Mainz, Germany and was introduced to the field of biophysical chemistry during her diploma work in the laboratory of Prof. Andreas Janshoff. For her doctoral research, she studied the structure and dynamics of the eukaryotic RNA polymerase II transcription initiation complex using single-molecule fluorescence techniques in the laboratory of Prof. Jens Michaelis at the Ludwig Maximilians-University München, Germany. After receiving her Ph.D. in 2012, she moved to Stanford for postdoctoral research with Prof. Stephen Quake studying cellular heterogeneity of complex tissues using single cell transcriptomics.

## ACKNOWLEDGMENTS

We thank Gray Camp and Julia Nagy for carefully proofreading the manuscript. J.M. was supported by an ERC starting grant.

## REFERENCES

- (1) Cramer, P.; Bushnell, D. A.; Fu, J.; Gnatt, A. L.; Maier-Davis, B.; Thompson, N. E.; Burgess, R. R.; Edwards, A. M.; David, P. R.; Kornberg, R. D. *Science* **2000**, *288*, 640.
- (2) Cramer, P.; Bushnell, D. A.; Kornberg, R. D. *Science* **2001**, *292*, 1863.
- (3) Cramer, P.; Armache, K.-J.; Baumli, S.; Benkert, S.; Brueckner, F.; Buchen, C.; Damsma, G. E.; Dengl, S.; Geiger, S. R.; Jasiak, A. J.; Jawhari, A.; Jennebach, S.; Kamenski, T.; Kettenberger, H.; Kuhn, C.-D.; Lehmann, E.; Leike, K.; Sydow, J. F.; Vannini, A. *Annu. Rev. Biophys.* **2008**, *37*, 337.
- (4) Armache, K.-J.; Kettenberger, H.; Cramer, P. *Proc. Natl. Acad. Sci. U.S.A.* **2003**, *100*, 6964.
- (5) Kettenberger, H.; Armache, K.-J.; Cramer, P. *Mol. Cell* **2004**, *16*, 955.
- (6) Bushnell, D. A.; Kornberg, R. D. *Proc. Natl. Acad. Sci. U.S.A.* **2003**, *100*, 6969.
- (7) Westover, K. D.; Bushnell, D. A.; Kornberg, R. D. *Science* **2004**, *303*, 1014.
- (8) Bushnell, D. A.; Westover, K. D.; Davis, R. E.; Kornberg, R. D. *Science* **2004**, *303*, 983.
- (9) Vassilyev, D. G.; Sekine, S.-I.; Laptenko, O.; Lee, J.; Vassilyeva, M. N.; Borukhov, S.; Yokoyama, S. *Nature* **2002**, *417*, 712.
- (10) Vassilyev, D. G.; Vassilyeva, M. N.; Zhang, J.; Palangat, M.; Artsimovitch, I.; Landick, R. *Nature* **2007**, *448*, 163.
- (11) Vassilyev, D. G.; Vassilyeva, M. N.; Perederina, A.; Tahirov, T. H.; Artsimovitch, I. *Nature* **2007**, *448*, 157.
- (12) Murakami, K. S.; Masuda, S.; Campbell, E. A.; Muzzin, O.; Darst, S. A. *Science* **2002**, *296*, 1285.
- (13) Cramer, P. *J. Mol. Biol.* **2008**, *376*, 303.
- (14) Ringel, R.; Sologub, M.; Morozov, Y. I.; Litonin, D.; Cramer, P.; Temiakov, D. *Nature* **2011**, *478*, 269.
- (15) Cheetham, G. M.; Jeruzalmi, D.; Steitz, T. A. *Nature* **1999**, *399*, 80.
- (16) Cheetham, G. M.; Steitz, T. A. *Science* **1999**, *286*, 2305.
- (17) Cheung, A. C. M.; Cramer, P. *Cell* **2012**, *149*, 1431.
- (18) Larson, D. R.; Singer, R. H.; Zenklusen, D. *Trends Cell Biol.* **2009**, *19*, 630.
- (19) Larson, M. H.; Landick, R.; Block, S. M. *Mol. Cell* **2011**, *41*, 249.
- (20) Darzacq, X.; Yao, J.; Larson, D. R.; Causse, S. Z.; Bosanac, L.; De Turre, V.; Ruda, V. M.; Lionnet, T.; Zenklusen, D.; Guglielmi, B.; Tjian, R.; Singer, R. H. *Annu. Rev. Biophys.* **2009**, *38*, 173.
- (21) Zhou, J.; Schweikhard, V.; Block, S. M. *Biochim. Biophys. Acta* **2013**, *1829*, 29.
- (22) Bai, L.; Santangelo, T. J.; Wang, M. D. *Annu. Rev. Biophys. Biomol. Struct.* **2006**, *35*, 343.
- (23) Joo, C.; Balci, H.; Ishitsuka, Y.; Buranachai, C.; Ha, T. *Annu. Rev. Biochem.* **2008**, *77*, 51.
- (24) Joo, C.; Fareh, M.; Kim, V. N. *Trends Biochem. Sci.* **2013**, *38*, 30.
- (25) Hohlbein, J.; Gryte, K.; Heilemann, M.; Kapanidis, A. N. *Phys. Biol.* **2010**, *7*, 031001.
- (26) Peterman, E. J. G.; Sosa, H.; Moerner, W. E. *Annu. Rev. Phys. Chem.* **2004**, *55*, 79.
- (27) Walter, N. G.; Huang, C.-Y.; Manzo, A. J.; Sobhy, M. A. *Nat. Methods* **2008**, *5*, 475.
- (28) Deniz, A.; Mukhopadhyay, S.; Lemke, E. J. *R. Soc. Interface* **2008**, *5*, 15.
- (29) Moerner, W.; Kador, L. *Phys. Rev. Lett.* **1989**, *62*, 2535.
- (30) Orrit, M.; Bernard, J. *Phys. Rev. Lett.* **1990**, *65*, 2716.
- (31) Funatsu, T.; Harada, Y.; Tokunaga, M.; Saito, K.; Yanagida, T. *Nature* **1995**, *374*, 555.
- (32) Zhuang, X. *Annu. Rev. Biophys. Biomol. Struct.* **2005**, *34*, 399.
- (33) Ha, T.; Kozlov, A. G.; Lohman, T. M. *Annu. Rev. Biophys.* **2012**, *41*, 295.
- (34) Finkelstein, I. J.; Greene, E. C. *Annu. Rev. Biophys.* **2012**, *42*, 130301134023003.
- (35) Park, H.; Toprak, E.; Selvin, P. R. *Q. Rev. Biophys.* **2007**, *40*, 87.
- (36) Toprak, E.; Selvin, P. R. *Annu. Rev. Biophys. Biomol. Struct.* **2007**, *36*, 349.
- (37) English, B. P.; Min, W.; van Oijen, A. M.; Lee, K. T.; Luo, G.; Sun, H.; Cherayil, B. J.; Kou, S. C.; Xie, X. S. *Nat. Chem. Biol.* **2006**, *2*, 87.
- (38) Engelkamp, H.; Hatzakis, N. S.; Hofkens, J.; De Schryver, F. C.; Nolte, R. J. M.; Rowan, A. E. *Chem. Commun.* **2006**, 935.
- (39) Eaton, W. *Curr. Opin. Struct. Biol.* **2008**, *18*, 16.
- (40) Schuler, B.; Lipman, E. A.; Eaton, W. A. *Nature* **2002**, *419*, 743.
- (41) Ulbrich, M. H.; Isacoff, E. Y. *Nat. Methods* **2007**, *4*, 319.
- (42) Shu, D. D.; Zhang, H. H.; Jin, J. J.; Guo, P. P. *EMBO J.* **2007**, *26*, 527.
- (43) Levene, M. J.; Korlach, J.; Turner, S. W.; Foquet, M.; Craighead, H. G.; Webb, W. W. *Science* **2003**, *299*, 682.
- (44) Zhu, P.; Craighead, H. G. *Annu. Rev. Biophys.* **2012**, *41*, 269.
- (45) Xie, X. S.; Choi, P. J.; Li, G.-W.; Lee, N. K.; Lia, G. *Annu. Rev. Biophys.* **2008**, *37*, 417.
- (46) Sakon, J.; Weninger, K. *Nat. Methods* **2010**, *7*, 203.
- (47) Schmidt, T.; Schütz, G. J.; Baumgartner, W.; Gruber, H. J.; Schindler, H. *Proc. Natl. Acad. Sci. U.S.A.* **1996**, *93*, 2926.
- (48) Cheezum, M. K.; Walker, W. F.; Guilford, W. H. *Biophys. J.* **2001**, *81*, 2378.
- (49) Seisenberger, G.; Ried, M. U.; Endress, T.; Büning, H.; Hallek, M.; Bräuchle, C. *Science* **2001**, *294*, 1929.
- (50) Michaelis, J.; Bräuchle, C. *Chem. Soc. Rev.* **2010**, *39*, 4731.
- (51) Hausteiner, E.; Schwille, P. *Annu. Rev. Biophys. Biomol. Struct.* **2007**, *36*, 151.

- (52) Lacoste, T. D.; Michalet, X.; Pinaud, F.; Chemla, D. S.; Alivisatos, A. P.; Weiss, S. *Proc. Natl. Acad. Sci. U.S.A.* **2000**, *97*, 9461.
- (53) Kohl, T.; Hausteiner, E.; Schwill, P. *Biophys. J.* **2005**, *89*, 2770.
- (54) Brustad, E. M.; Lemke, E. A.; Schultz, P. G.; Deniz, A. A. *J. Am. Chem. Soc.* **2008**, *130*, 17664.
- (55) Yin, J.; Lin, A. J.; Golan, D. E.; Walsh, C. T. *Nat. Protoc.* **2006**, *1*, 280.
- (56) Becker, C.; Seidel, R.; Jahnz, M.; Bacia, K.; Niederhausen, T.; Alexandrov, K.; Schwill, P.; Goody, R.; Engelhard, M. *ChemBioChem* **2006**, *7*, 891.
- (57) Gramlich, P. M. E.; Wirges, C. T.; Manetto, A.; Carell, T. *Angew. Chem., Int. Ed.* **2008**, *47*, 8350.
- (58) Yang, J.; Yang, W. *J. Am. Chem. Soc.* **2009**, *131*, 11644.
- (59) Best, M. D. *Biochemistry* **2009**, *48*, 6571.
- (60) Uttamapinant, C.; White, K. A.; Baruah, H.; Thompson, S.; Fernández-Suárez, M.; Puthenveetil, S.; Ting, A. Y. *Proc. Natl. Acad. Sci. U.S.A.* **2010**, *107*, 10914.
- (61) Milles, S.; Lemke, E. A. *BioEssays* **2012**, *35*, 65.
- (62) Shi, X.; Jung, Y.; Lin, L.-J.; Liu, C.; Wu, C.; Cann, I. K. O.; Ha, T. *Nat. Methods* **2012**, *9*, 499.
- (63) Boukobza, E.; Sonnenfeld, A.; Haran, G. *J. Phys. Chem. B* **2001**, *105*, 12165.
- (64) Pal, P.; Lesoine, J. F.; Lieb, M. A.; Novotny, L.; Knauf, P. A. *Biophys. J.* **2005**, *89*, L11.
- (65) Liu, B.; Mazouchi, A.; Gradinaru, C. C. *J. Phys. Chem. B* **2010**, *114*, 15191.
- (66) Rasnik, I.; McKinney, S. A.; Ha, T. *Acc. Chem. Res.* **2005**, *38*, 542.
- (67) Jung, C.; Müller, B. K.; Lamb, D. C.; Nolde, F.; Müllen, K.; Bräuchle, C. *J. Am. Chem. Soc.* **2006**, *128*, 5283.
- (68) Jung, C.; Ruthardt, N.; Lewis, R.; Michaelis, J.; Sodeik, B.; Nolde, F.; Peneva, K.; Müllen, K.; Bräuchle, C. *ChemPhysChem* **2009**, *10*, 180.
- (69) Altman, R. B.; Terry, D. S.; Zhou, Z.; Zheng, Q.; Geggier, P.; Kolster, R. A.; Zhao, Y.; Javitch, J. A.; Warren, J. D.; Blanchard, S. C. *Nat. Methods* **2011**, *9*, 68.
- (70) Ha, T.; Tinnefeld, P. *Annu. Rev. Phys. Chem.* **2012**, *63*, 595.
- (71) Cordes, T.; Vogelsang, J.; Tinnefeld, P. *J. Am. Chem. Soc.* **2009**, *131*, 5018.
- (72) Rasnik, I.; McKinney, S. A.; Ha, T. *Nat. Methods* **2006**, *3*, 891.
- (73) Hohng, S.; Ha, T. *J. Am. Chem. Soc.* **2004**, *126*, 1324.
- (74) Courty, S.; Luccardini, C.; Bellaiche, Y.; Cappello, G.; Dahan, M. *Nano Lett.* **2006**, *6*, 1491.
- (75) Leduc, C.; Ruhnnow, F.; Howard, J.; Diez, S. *Proc. Natl. Acad. Sci. U.S.A.* **2007**, *104*, 10847.
- (76) Zheng, J.; Nicovich, P. R.; Dickson, R. M. *Annu. Rev. Phys. Chem.* **2007**, *58*, 409.
- (77) Neugart, F.; Zappe, A.; Jelezko, F.; Tietz, C.; Boudou, J. P.; Krueger, A.; Wrachtrup, J. *Nano Lett.* **2007**, *7*, 3588.
- (78) Zhuang, X. *Nature Publishing Group* **2009**, *3*, 365.
- (79) Huang, B.; Wang, W.; Bates, M.; Zhuang, X. *Science* **2008**, *319*, 810.
- (80) Dempsey, G. T.; Vaughan, J. C.; Chen, K. H.; Bates, M.; Zhuang, X. *Nat. Methods* **2011**, *8*, 1027.
- (81) Bates, M.; Huang, B.; Dempsey, G. T.; Zhuang, X. *Science* **2007**, *317*, 1749.
- (82) Huang, B.; Bates, M.; Zhuang, X. *Annu. Rev. Biochem.* **2009**, *78*, 993.
- (83) Betzig, E.; Patterson, G. H.; Sougrat, R.; Lindwasser, O. W.; Olenych, S.; Bonifacino, J. S.; Davidson, M. W.; Lippincott-Schwartz, J.; Hess, H. F. *Science* **2006**, *313*, 1642.
- (84) Manley, S.; Gillette, J.; Patterson, G.; Shroff, H.; Hess, H.; Betzig, E.; Lippincott-Schwartz, J. *Nat. Methods* **2008**, *5*, 155.
- (85) Patterson, G.; Davidson, M.; Manley, S.; Lippincott-Schwartz, J. *Annu. Rev. Phys. Chem.* **2010**, *61*, 345.
- (86) Hess, S. T.; Girirajan, T. P. K.; Mason, M. D. *Biophys. J.* **2008**, *91*, 4258.
- (87) Heilemann, M.; van de Linde, S.; Mukherjee, A.; Sauer, M. *Angew. Chem., Int. Ed.* **2009**, *48*, 6903.
- (88) Ha, T.; Ting, A.; Liang, J.; Deniz, A.; Chemla, D.; Schultz, P.; Weiss, S. *Chem. Phys.* **1999**, *247*, 107.
- (89) Deniz, A. A.; Dahan, M.; Grunwell, J. R.; Ha, T.; Faulhaber, A. E.; Chemla, D. S.; Weiss, S.; Schultz, P. G. *Proc. Natl. Acad. Sci. U.S.A.* **1999**, *96*, 3670.
- (90) Ha, T.; Ting, A. Y.; Liang, J.; Caldwell, W. B.; Deniz, A. A.; Chemla, D. S.; Schultz, P. G.; Weiss, S. *Proc. Natl. Acad. Sci. U.S.A.* **1999**, *96*, 893.
- (91) Selvin, P. R. *Nat. Struct. Biol.* **2000**, *7*, 730.
- (92) Roy, R.; Hohng, S.; Ha, T. *Nat. Methods* **2008**, *5*, 507.
- (93) Lilley, D.; Wilson, T. *Curr. Opin. Chem. Biol.* **2000**, *4*, 507.
- (94) Förster, T. *Ann. Phys. (Berlin, Ger.)* **1948**, *437*, 55.
- (95) Stryer, L.; Haugland, R. P. *Proc. Natl. Acad. Sci. U.S.A.* **1967**, *58*, 719.
- (96) Sabanayagam, C. R.; Eid, J. S.; Meller, A. *J. Chem. Phys.* **2005**, *122*, 061103.
- (97) Torres, T.; Levitus, M. *J. Phys. Chem. B* **2007**, *111*, 7392.
- (98) Lewis, R.; Dürr, H.; Hopfner, K.-P.; Michaelis, J. *Nucleic Acids Res.* **2008**, *36*, 1881.
- (99) Yang, H.; Luo, G.; Karnchanaphanurach, P.; Louie, T.-M.; Rech, I.; Cova, S.; Xun, L.; Xie, X. S. *Science* **2003**, *302*, 262.
- (100) Antonik, M.; Felekyan, S.; Gaiduk, A.; Seidel, C. A. M. *J. Phys. Chem. B* **2006**, *110*, 6970.
- (101) Santoso, Y.; Torella, J. P.; Kapanidis, A. N. *ChemPhysChem* **2010**, *11*, 2209.
- (102) Kudryavtsev, V.; Felekyan, S.; Woźniak, A. K.; König, M.; Sandhagen, C.; Kühnemuth, R.; Seidel, C. A. M.; Oesterheld, F. *Anal. Bioanal. Chem.* **2007**, *387*, 71.
- (103) Müller, B. K.; Zaychikov, E.; Bräuchle, C.; Lamb, D. C. *Biophys. J.* **2005**, *89*, 3508.
- (104) Lee, N. K.; Kapanidis, A. N.; Wang, Y.; Michalet, X.; Mukhopadhyay, J.; Ebricht, R. H.; Weiss, S. *Biophys. J.* **2005**, *88*, 2939.
- (105) Sindbert, S.; Kalinin, S.; Nguyen, H.; Kienzler, A.; Klima, L.; Bannwarth, W.; Appel, B.; Müller, S.; Seidel, C. A. M. *J. Am. Chem. Soc.* **2011**, *133*, 2463.
- (106) Michaelis, J. In *Single Particle Tracking and Single Molecule Energy Transfer*; Wiley-VCH Verlag GmbH & Co. KGaA: Weinheim, Germany, 2009; pp 191–214.
- (107) Kalinin, S.; Peulen, T.; Sindbert, S.; Rothwell, P. J.; Berger, S.; Restle, T.; Goody, R. S.; Gohlke, H.; Seidel, C. A. M. *Nat. Methods* **2012**, *9*, 1218.
- (108) Andrecka, J.; Treutlein, B.; Arcusa, M. A. I.; Muschiello, A.; Lewis, R.; Cheung, A. C. M.; Cramer, P.; Michaelis, J. *Nucleic Acids Res.* **2009**, *37*, 5803.
- (109) Muschiello, A.; Andrecka, J.; Jawhari, A.; Brückner, F.; Cramer, P.; Michaelis, J. *Nat. Methods* **2008**, *5*, 965.
- (110) Muschiello, A.; Michaelis, J. *J. Phys. Chem. B* **2011**, *115*, 11927.
- (111) Rasnik, I.; Myong, S.; Cheng, W.; Lohman, T. M.; Ha, T. *J. Mol. Biol.* **2004**, *336*, 395.
- (112) Choi, U. B.; Strop, P.; Vrljic, M.; Chu, S.; Brunger, A. T.; Weninger, K. R. *Nat. Struct. Mol. Biol.* **2010**, *17*, 318.
- (113) Andrecka, J.; Lewis, R.; Brückner, F.; Lehmann, E.; Cramer, P.; Michaelis, J. *Proc. Natl. Acad. Sci. U.S.A.* **2008**, *105*, 135.
- (114) Bustamante, C.; Chemla, Y. R.; Forde, N. R.; Izhaky, D. *Annu. Rev. Biochem.* **2004**, *73*, 705.
- (115) Puchner, E. M.; Gaub, H. E. *Annu. Rev. Biophys.* **2012**, *41*, 497.
- (116) Janshoff, A.; Neitzert, M.; Oberdörfer, Y.; Fuchs, H. *Angew. Chem., Int. Ed.* **2000**, *39*, 3212.
- (117) Carrion-Vazquez, M.; Oberhauser, A. F.; Fisher, T. E.; Marszalek, P. E.; Li, H.; Fernandez, J. M. *Prog. Biophys. Mol. Biol.* **2000**, *74*, 63.
- (118) Yanagida, T.; Esaki, S.; Iwane, A. H.; Inoue, Y.; Ishijima, A.; Kitamura, K.; Tanaka, H.; Tokunaga, M. *Philos. Trans. R. Soc., B* **2000**, *355*, 441.
- (119) Moffitt, J. R.; Chemla, Y. R.; Smith, S. B.; Bustamante, C. *Annu. Rev. Biochem.* **2008**, *77*, 205.
- (120) Svoboda, K.; Block, S. M. *Annu. Rev. Biophys. Biomol. Struct.* **1994**, *23*, 247.
- (121) Neuman, K. C.; Block, S. M. *Rev. Sci. Instrum.* **2004**, *75*, 2787.

- (122) Greenleaf, W. J.; Woodside, M. T.; Block, S. M. *Annu. Rev. Biophys. Biomol. Struct.* **2007**, *36*, 171.
- (123) Neuman, K.; Nagy, A. *Nat. Methods* **2008**, *5*, 491.
- (124) De Vlaminck, I.; Dekker, C. *Annu. Rev. Biophys.* **2012**, *41*, 453.
- (125) Block, S. M. *Nature* **1992**, *360*, 493.
- (126) Ashkin, A. *Phys. Rev. Lett.* **1970**, *24*, 156.
- (127) Ashkin, A.; Dziedzic, J. M.; Bjorkholm, J. E.; Chu, S. *Opt. Lett.* **1986**, *11*, 288.
- (128) Molloy, J.; Padgett, M. *Contemp. Phys.* **2002**, *43*, 241.
- (129) Nugent-Glandorf, L.; Perkins, T. T. *Opt. Lett.* **2004**, *29*, 2611.
- (130) Meiners, J. C.; Quake, S. R. *Phys. Rev. Lett.* **2000**, *84*, 5014.
- (131) Kapanidis, A. N.; Margeat, E.; Ho, S. O.; Kortkhonjia, E.; Weiss, S.; Ebricht, R. H. *Science* **2006**, *314*, 1144.
- (132) Abbondanzieri, E. A.; Greenleaf, W. J.; Shaevitz, J. W.; Landick, R.; Block, S. M. *Nature* **2005**, *438*, 460.
- (133) Moffitt, J. R.; Chemla, Y. R.; Izhaky, D.; Bustamante, C. *Proc. Natl. Acad. Sci. U.S.A.* **2006**, *103*, 9006.
- (134) Berg-Sørensen, K.; Flyvbjerg, H. *Rev. Sci. Instrum.* **2004**, *75*, 594.
- (135) Berg-Sørensen, K.; Peterman, E. J.; Weber, T.; Schmidt, C. F.; Flyvbjerg, H. *Rev. Sci. Instrum.* **2006**, *77*, 063106.
- (136) Bustamante, C.; Bryant, Z.; Smith, S. B. *Nature* **2003**, 423.
- (137) Smith, S. B.; Cui, Y.; Bustamante, C. *Science* **1996**, *271*, 795.
- (138) Marko, J. F. *Phys. Rev. E* **1998**, *57*, 2134.
- (139) Shundrovsky, A. A.; Santangelo, T. J. T.; Roberts, J. W. J.; Wang, M. D. M. *Biophys. J.* **2004**, *87*, 9.
- (140) Yin, H. H.; Landick, R. R.; Gelles, J. J. *Biophys. J.* **1994**, *67*, 11.
- (141) Lyubchenko, Y. L.; Shlyakhtenko, L. S.; Ando, T. *Methods* **2011**, *54*, 274.
- (142) Bustamante, C. C.; Rivetti, C. C. *Annu. Rev. Biophys. Biomol. Struct.* **1995**, *25*, 395.
- (143) Binnig, G.; Quate, C.; Gerber, C. *Phys. Rev. Lett.* **1986**, *56*, 930.
- (144) Vesenska, J.; Guthold, M.; Tang, C. L.; Keller, D.; Delaine, E.; Bustamante, C. *Ultramicroscopy* **1992**, *42–44*, 1243.
- (145) Rivetti, C.; Guthold, M.; Bustamante, C. *J. Mol. Biol.* **1996**, *264*, 919.
- (146) Rees, W.; Keller, R.; Vesenska, J.; Yang, G.; Bustamante, C. *Science* **1993**, *260*, 1646.
- (147) Rivetti, C.; Codeluppi, S.; Dieci, G.; Bustamante, C. *J. Mol. Biol.* **2003**, *326*, 1413.
- (148) Rivetti, C. C.; Guthold, M. M.; Bustamante, C. C. *EMBO J.* **1999**, *18*, 4464.
- (149) Guthold, M. M.; Zhu, X. X.; Rivetti, C. C.; Yang, G. G.; Thomson, N. H. N.; Kasas, S. S.; Hansma, H. G. H.; Smith, B. B.; Hansma, P. K. P.; Bustamante, C. C. *Biophys. J.* **1999**, *77*, 11.
- (150) Guthold, M. M.; Bezanilla, M. M.; Erie, D. A. D.; Jenkins, B. B.; Hansma, H. G. H.; Bustamante, C. C. *Proc. Natl. Acad. Sci. U.S.A.* **1994**, *91*, 12927.
- (151) Ando, T. *Nanotechnology* **2012**, *23*, 062001.
- (152) Kodera, N.; Yamamoto, D.; Ishikawa, R.; Ando, T. *Nature* **2010**, 1.
- (153) Uchihashi, T.; Iino, R.; Ando, T.; Noji, H. *Science* **2011**, *333*, 755.
- (154) Bertrand, E. E.; Chartrand, P. P.; Schaefer, M. M.; Shenoy, S. M. S.; Singer, R. H. R.; Long, R. M. R. *Mol. Cell* **1998**, *2*, 9.
- (155) Femino, A. M. *Science* **1998**, *280*, 585.
- (156) Itzkovitz, S.; Van Oudenaarden, A. *Nat. Methods* **2011**, *8*, S12.
- (157) Itzkovitz, S.; Lyubimova, A.; Blat, I. C.; Maynard, M.; van Es, J.; Lees, J.; Jacks, T.; Clevers, H.; Van Oudenaarden, A. *Nat. Cell Biol.* **2011**, *14*, 106.
- (158) Hocine, S.; Raymond, P.; Zenklusen, D.; Chao, J. A.; Singer, R. H. *Nat. Methods* **2012**, 1.
- (159) Raj, A.; Peskin, C. S.; Tranchina, D.; Vargas, D. Y.; Tyagi, S. *PLoS Biol.* **2006**, *4*, e309.
- (160) Raj, A.; Rifkin, S. A.; Andersen, E.; Van Oudenaarden, A. *Nature* **2010**, *463*, 913.
- (161) So, L.-H.; Ghosh, A.; Zong, C.; Sepúlveda, L. A.; Segev, R.; Golding, I. *Nat. Genet.* **2011**, *43*, 554.
- (162) Larson, D. R.; Zenklusen, D.; Wu, B.; Chao, J. A.; Singer, R. H. *Science* **2011**, *332*, 475.
- (163) Bertrand, E.; Chartrand, P.; Schaefer, M.; Shenoy, S. M.; Singer, R. H.; Long, R. M. *Mol. Cell* **1998**, *2*, 437.
- (164) Golding, I.; Paulsson, J.; Zawilski, S. M.; Cox, E. C. *Cell* **2005**, *123*, 1025.
- (165) Golding, I. *Proc. Natl. Acad. Sci. U.S.A.* **2004**, *101*, 11310.
- (166) Yunger, S.; Rosenfeld, L.; Garini, Y.; Shav-Tal, Y. *Nat. Methods* **2010**, *7*, 631.
- (167) Yunger, S.; Rosenfeld, L.; Garini, Y.; Shav-Tal, Y. *Nat. Protoc.* **2013**, *8*, 393.
- (168) Lionnet, T.; Czaplinski, K.; Darzacq, X.; Shav-Tal, Y.; Wells, A. L.; Chao, J. A.; Park, H. Y.; De Turrís, V.; Lopez-Jones, M.; Singer, R. H. *Nat. Methods* **2011**, *8*, 165.
- (169) Treutlein, B.; Michaelis, J. *Angew. Chem., Int. Ed.* **2011**, *50*, 9788.
- (170) Darzacq, X.; Shav-Tal, Y.; De Turrís, V.; Brody, Y.; Shenoy, S. M.; Phair, R. D.; Singer, R. H. *Nat. Struct. Mol. Biol.* **2007**, *14*, 796.
- (171) Janicki, S. M.; Tsukamoto, T.; Salghetti, S. E.; Tansey, W. P.; Sachidanandam, R.; Prasanth, K. V.; Ried, T.; Shav-Tal, Y.; Bertrand, E.; Singer, R. H.; Spector, D. L. *Cell* **2004**, *116*, 683.
- (172) Chubb, J. R.; Trcek, T.; Shenoy, S. M.; Singer, R. H. *Curr. Biol.* **2006**, *16*, 1018.
- (173) Bedell, V. M.; Wang, Y.; Campbell, J. M.; Poshusta, T. L.; Starker, C. G.; Krug, R. G., II; Tan, W.; Penheiter, S. G.; Ma, A. C.; Leung, A. Y. H.; Fahrenkrug, S. C.; Carlson, D. F.; Voytas, D. F.; Clark, K. J.; Essner, J. J.; Ekker, S. C. *Nature* **2012**, *491*, 114.
- (174) Mali, P.; Yang, L.; Esvelt, K. M.; Aach, J.; Guell, M.; DiCarlo, J. E.; Norville, J. E.; Church, G. M. *Science* **2013**, *339*, 823.
- (175) Tyagi, S.; Kramer, F. R. *Nat. Biotechnol.* **1996**, *14*, 303.
- (176) Bratu, D. P.; Cha, B.-J.; Mhlanga, M. M.; Kramer, F. R.; Tyagi, S. *Proc. Natl. Acad. Sci. U.S.A.* **2003**, *100*, 13308.
- (177) Vargas, D. Y.; Shah, K.; Batish, M.; Levandoski, M.; Sinha, S.; Marras, S. A. E.; Schedl, P.; Tyagi, S. *Cell* **2011**, *147*, 1054.
- (178) Vargas, D. Y.; Raj, A.; Marras, S. A. E.; Kramer, F. R.; Tyagi, S. *Proc. Natl. Acad. Sci. U.S.A.* **2005**, *102*, 17008.
- (179) Gebhardt, J. C. M.; Suter, D. M.; Roy, R.; Zhao, Z. W.; Chapman, A. R.; Basu, S.; Maniatis, T.; Xie, X. S. *Nat. Methods* **2013**, *10*, 421.
- (180) Brody, Y.; Neufeld, N.; Bieberstein, N.; Causse, S. Z.; Böhlein, E.-M.; Neugebauer, K. M.; Darzacq, X.; Shav-Tal, Y. *PLoS Biol.* **2011**, *9*, e1000573.
- (181) Ujvári, A.; Luse, D. S. *Nature Publishing Group* **2005**, *13*, 49.
- (182) Schaefer, D. A.; Gelles, J.; Sheetz, M. P.; Landick, R. *Nature* **1991**, *352*, 444.
- (183) Kabata, H.; Kurosawa, O.; Arai, I.; Washizu, M.; Margaron, S. A.; Glass, R. E.; Shimamoto, N. *Science* **1993**, *262*, 1561.
- (184) Harada, Y.; Ohara, O.; Takatsuki, A.; Itoh, H.; Shimamoto, N.; Kinoshita, K. *Nature* **2001**, *409*, 113.
- (185) Gelles, J.; Landick, R. *Cell* **1998**, *93*, 13.
- (186) Wang, M. D.; Schnitzer, M. J.; Yin, H.; Landick, R.; Gelles, J.; Block, S. M. *Science* **1998**, *282*, 902.
- (187) Wang, H. Y.; Elston, T.; Mogilner, A.; Oster, G. *Biophys. J.* **1998**, *74*, 1186.
- (188) Yin, H.; Wang, M. D.; Svoboda, K.; Landick, R.; Block, S. M.; Gelles, J. *Science* **1995**, *270*, 1653.
- (189) Thomen, P.; Lopez, P. J.; Heslot, F. *Phys. Rev. Lett.* **2005**, *94*, 128102.
- (190) Shaevitz, J. W.; Abbondanzieri, E. A.; Landick, R.; Block, S. M. *Nature* **2003**, *426*, 684.
- (191) Greenleaf, W. J.; Woodside, M. T.; Abbondanzieri, E. A.; Block, S. M. *Phys. Rev. Lett.* **2005**, *95*, 208102.
- (192) Greenleaf, W. J.; Block, S. M. *Science* **2006**, *313*, 801.
- (193) Tolic-Nørrelykke, S. F.; Engh, A. M.; Landick, R.; Gelles, J. J. *Biol. Chem.* **2004**, *279*, 3292.
- (194) Adelman, K. K.; La Porta, A. A.; Santangelo, T. J. T.; Lis, J. T. J.; Roberts, J. W. J.; Wang, M. D. M. *Proc. Natl. Acad. Sci. U.S.A.* **2002**, *99*, 13538.

- (195) Thomen, P.; Lopez, P.; Bockelmann, U.; Guillerez, J.; Dreyfus, M.; Heslot, F. *Biophys. J.* **2008**, *95*, 2423.
- (196) Larson, M. H.; Zhou, J.; Kaplan, C. D.; Palangat, M.; Kornberg, R. D.; Landick, R.; Block, S. M. *Proc. Natl. Acad. Sci. U.S.A.* **2012**, *109*, 6555.
- (197) Davenport, R. J.; Wuite, G. J.; Landick, R.; Bustamante, C. *Science* **2000**, *287*, 2497.
- (198) Neuman, K. C.; Abbondanzieri, E. A.; Landick, R.; Gelles, J.; Block, S. M. *Cell* **2003**, *115*, 437.
- (199) Herbert, K. M.; La Porta, A.; Wong, B. J.; Mooney, R. A.; Neuman, K. C.; Landick, R.; Block, S. M. *Cell* **2006**, *125*, 1083.
- (200) Forde, N. R.; Izhaky, D.; Woodcock, G. R.; Wuite, G. J.; Bustamante, C. *Proc. Natl. Acad. Sci. U.S.A.* **2002**, *99*, 11682.
- (201) Bai, L.; Fulbright, R. M.; Wang, M. D. *Phys. Rev. Lett.* **2007**, *98*, 068103.
- (202) Galburt, E.; Grill, S.; Bustamante, C. *Methods* **2009**, *48*, 323.
- (203) Galburt, E. A.; Grill, S. W.; Wiedmann, A.; Lubkowska, L.; Choy, J.; Nogales, E.; Kashlev, M.; Bustamante, C. *Nature* **2007**, *446*, 820.
- (204) Depken, M.; Galburt, E.; Grill, S.; Kireeva, M.; Hancock, B.; Cremona, G.; Walter, W.; Studitsky, V.; Kashlev, M. *Biophys. J.* **2009**, *96*, 2189.
- (205) Zamft, B. B.; Bintu, L. L.; Ishibashi, T. T.; Bustamante, C. C. *Proc. Natl. Acad. Sci. U.S.A.* **2012**, *109*, 8948.
- (206) Ninio, J. J. *Biochimie* **1991**, *73*, 1517.
- (207) Sydow, J. F.; Cramer, P. *Curr. Opin. Struct. Biol.* **2009**, *19*, 732.
- (208) Sydow, J.; Brueckner, F.; Cheung, A.; Damsma, G.; Dengl, S.; Lehmann, E.; Vassilyev, D.; Cramer, P. *Mol. Cell* **2009**, *34*, 710.
- (209) Brueckner, F.; Hennecke, U.; Carell, T.; Cramer, P. *Science* **2007**, *315*, 859.
- (210) Wang, D.; Bushnell, D.; Huang, X.; Westover, K.; Levitt, M.; Kornberg, R. *Science* **2009**, *324*, 1203.
- (211) Cheung, A. C. M.; Cramer, P. *Nature* **2011**, *471*, 249.
- (212) Walmacq, C.; Cheung, A. C. M.; Kireeva, M. L.; Lubkowska, L.; Ye, C.; Gotte, D.; Strathern, J. N.; Carell, T.; Cramer, P.; Kashlev, M. *Mol. Cell* **2012**, *46*, 18.
- (213) Kettenberger, H.; Armache, K.-J.; Cramer, P. *Cell* **2003**, *114*, 347.
- (214) Zhang, C.; Burton, Z. F. *J. Mol. Biol.* **2004**, *342*, 1085.
- (215) Grohmann, D.; Nagy, J.; Chakraborty, A.; Klose, D.; Fielden, D.; Ebright, R. H.; Michaelis, J.; Werner, F. *Mol. Cell* **2011**, *43*, 263.
- (216) Martinez-Rucobo, F. W.; Sainsbury, S.; Cheung, A. C. M.; Cramer, P. *EMBO J.* **2011**, *30*, 1302.
- (217) Erie, D. A.; Hajiseyedjavadi, O.; Young, M. C.; von Hippel, P. H. *Science* **1993**, *262*, 867.
- (218) Artsimovitch, I.; Landick, R. *Proc. Natl. Acad. Sci. U.S.A.* **2000**, *97*, 7090.
- (219) Opalka, N.; Chlenov, M.; Chacon, P.; Rice, W. J.; Wriggers, W.; Darst, S. A. *Cell* **2003**, *114*, 335.
- (220) Touloukhonov, I.; Zhang, J.; Palangat, M.; Landick, R. *Mol. Cell* **2007**, *27*, 406.
- (221) Wang, D.; Bushnell, D. A.; Westover, K. D.; Kaplan, C. D.; Kornberg, R. D. *Cell* **2006**, *127*, 941.
- (222) Da, L.-T.; Wang, D.; Huang, X. *J. Am. Chem. Soc.* **2012**, *134*, 2399.
- (223) Zhang, J.; Palangat, M.; Landick, R. *Nat. Struct. Mol. Biol.* **2009**, *17*, 99.
- (224) Kaplan, C.; Larsson, K.; Kornberg, R. *Mol. Cell* **2008**, *30*, 547.
- (225) Kireeva, M.; Nedialkov, Y.; Cremona, G.; Purtov, Y.; Lubkowska, L.; Malagon, F.; Burton, Z.; Strathern, J.; Kashlev, M. *Mol. Cell* **2008**, *30*, 557.
- (226) Kaplan, C. D.; Larsson, K.-M.; Kornberg, R. D. *Mol. Cell* **2008**, *30*, 547.
- (227) Li, B.; Carey, M.; Workman, J. L. *Cell* **2007**, *128*, 707.
- (228) Owen-Hughes, T.; Gkikopoulos, T. *Curr. Opin. Cell Biol.* **2012**, *24*, 296.
- (229) Fuchs, S. M.; Larabee, R. N.; Strahl, B. D. *Biochim. Biophys. Acta* **2009**, *1789*, 26.
- (230) Jenuwein, T. *Science* **2001**, *293*, 1074.
- (231) Becker, P. B.; Hörz, W. *Annu. Rev. Biochem.* **2002**, *71*, 247.
- (232) Saha, A.; Wittmeyer, J.; Cairns, B. *Nat. Rev. Mol. Cell Biol.* **2006**, *7*, 437.
- (233) Clapier, C.; Cairns, B. *Annu. Rev. Biochem.* **2009**, *78*, 273.
- (234) Flaus, A. A.; Owen-Hughes, T. T. *FEBS J.* **2011**, *278*, 3579.
- (235) Luger, K.; Mäder, A. W.; Richmond, R. K.; Sargent, D. F.; Richmond, T. J. *Nature* **1997**, *389*, 251.
- (236) Lowary, P. T. P.; Widom, J. J. *J. Mol. Biol.* **1998**, *276*, 24.
- (237) Widom, J. Q. *Rev. Biophys.* **2001**, *34*, 269.
- (238) Vasudevan, D.; Chua, E. Y. D.; Davey, C. A. *J. Mol. Biol.* **2010**, *403*, 1.
- (239) Bohm, V.; Hieb, A. R.; Andrews, A. J.; Gansen, A.; Rocker, A.; Tóth, K.; Luger, K.; Langowski, J. *Nucleic Acids Res.* **2011**, *39*, 3093.
- (240) Gansen, A.; Valeri, A.; Hauger, F.; Felekyan, S.; Kalinin, S.; Tóth, K.; Langowski, J.; Seidel, C. A. M. *Proc. Natl. Acad. Sci. U.S.A.* **2009**, *106*, 15308.
- (241) Koopmans, W. J. A.; Buning, R.; Schmidt, T.; van Noort, J. *Biophys. J.* **2009**, *97*, 195.
- (242) Li, G.; Levitus, M.; Bustamante, C.; Widom, J. *Nature Publishing Group* **2005**, *12*, 46.
- (243) Bonisch, C.; Schneider, K.; Punzeler, S.; Wiedemann, S. M.; Bielmeier, C.; Boccola, M.; Eberl, H. C.; Kuegel, W.; Neumann, J.; Kremmer, E.; Leonhardt, H.; Mann, M.; Michaelis, J.; Schermelleh, L.; Hake, S. B. *Nucleic Acids Res.* **2012**, *40*, 5951.
- (244) Brower-Toland, B.; Wang, M. D. *Methods Enzymol.* **2004**, *376*, 62.
- (245) Mihardja, S.; Spakowitz, A. J.; Zhang, Y.; Bustamante, C. *Proc. Natl. Acad. Sci. U.S.A.* **2006**, *103*, 15871.
- (246) Bennink, M. L.; Leuba, S. H.; Leno, G. H.; Zlatanova, J.; de Grooth, B. G.; Greve, J. *Nature Publishing Group* **2001**, *8*, 606.
- (247) Brower-Toland, B. D. B.; Smith, C. L. C.; Yeh, R. C. R.; Lis, J. T. J.; Peterson, C. L. C.; Wang, M. D. M. *Proc. Natl. Acad. Sci. U.S.A.* **2002**, *99*, 1960.
- (248) Hall, M.; Shundrovsky, A.; Bai, L.; Fulbright, R.; Lis, J.; Wang, M. *Nat. Struct. Mol. Biol.* **2009**, *16*, 124.
- (249) Killian, J. L.; Li, M.; Sheinin, M. Y.; Wang, M. D. *Curr. Opin. Struct. Biol.* **2012**.
- (250) Kireeva, M. L.; Walter, W.; Tchernajenko, V.; Bondarenko, V.; Kashlev, M.; Studitsky, V. M. *Mol. Cell* **2002**, *9*, 541.
- (251) Bondarenko, V.; Steele, L.; Újvári, A.; Gaykalova, D.; Kulaeva, O.; Polikanov, Y.; Luse, D.; Studitsky, V. M. *Mol. Cell* **2006**, *24*, 469.
- (252) Újvári, A.; Hsieh, F.-K.; Luse, S. W.; Studitsky, V. M.; Luse, D. S. *J. Biol. Chem.* **2008**, *283*, 32236.
- (253) Kireeva, M. L.; Hancock, B.; Cremona, G. H.; Walter, W.; Studitsky, V. M.; Kashlev, M. *Mol. Cell* **2005**, *18*, 97.
- (254) Luse, D. S.; Studitsky, V. M. *RNA Biol.* **2011**, *8*, 581.
- (255) Hsieh, F.-K.; Fisher, M.; Ri, A. U. J. A.; Studitsky, V. M.; Luse, D. S. *EMBO Rep.* **2010**, *11*, 705.
- (256) Luse, D. S.; Spangler, L. C.; Újvári, A. *J. Biol. Chem.* **2011**, *286*, 6040.
- (257) Hodges, C.; Bintu, L.; Lubkowska, L.; Kashlev, M.; Bustamante, C. *Science* **2009**, *325*, 626.
- (258) Bintu, L.; Ishibashi, T.; Dangkulwanich, M.; Wu, Y.-Y.; Lubkowska, L.; Kashlev, M.; Bustamante, C. *Cell* **2012**, *151*, 738.
- (259) Jin, J.; Bai, L.; Johnson, D. S.; Fulbright, R. M.; Kireeva, M. L.; Kashlev, M.; Wang, M. D. *Nature Publishing Group* **2010**, *17*, 745.
- (260) Bintu, L.; Kopaczynska, M.; Hodges, C.; Lubkowska, L.; Kashlev, M.; Bustamante, C. *Nat. Struct. Mol. Biol.* **2011**, *18*, 1394.
- (261) Cheung, A. C. M.; Sainsbury, S.; Cramer, P. *EMBO J.* **2011**, *30*, 4755.
- (262) Sainsbury, S.; Niesser, J.; Cramer, P. *Nature* **2013**, *493*, 437.
- (263) Zhang, Y.; Feng, Y.; Chatterjee, S.; Tuske, S.; Ho, M. X.; Arnold, E.; Ebright, R. H. *Science* **2012**, *338*, 1076.
- (264) Liu, X.; Bushnell, D. A.; Wang, D.; Calero, G.; Kornberg, R. D. *Science* **2010**, *327*, 206.
- (265) Kostrewa, D.; Zeller, M.; Armache, K.; Seizl, M.; Leike, K.; Thomm, M.; Cramer, P. *Nature* **2009**, *462*, 323.
- (266) He, Y.; Fang, J.; Taatjes, D. J.; Nogales, E. *Nature* **2013**, *495*, 481.

- (267) Tang, G.-Q.; Roy, R.; Bandwar, R. P.; Ha, T.; Patel, S. S. *Proc. Natl. Acad. Sci. U.S.A.* **2009**, *106*, 22175.
- (268) Sorokina, M.; Koh, H. R.; Patel, S. S.; Ha, T. *J. Am. Chem. Soc.* **2009**, *131*, 9630.
- (269) Revyakin, A.; Liu, C.; Ebright, R. H.; Strick, T. R. *Science* **2006**, *314*, 1139.
- (270) Strick, T.; Allemand, J.; Croquette, V.; Bensimon, D. *Prog. Biophys. Mol. Biol.* **2000**, *74*, 115.
- (271) Revyakin, A. A.; Ebright, R. H. R.; Strick, T. R. T. *Proc. Natl. Acad. Sci. U.S.A.* **2004**, *101*, 4776.
- (272) Robb, N. C.; Cordes, T.; Hwang, L. C.; Gryte, K.; Duchi, D.; Craggs, T. D.; Santoso, Y.; Weiss, S.; Ebright, R. H.; Kapanidis, A. N. *J. Mol. Biol.* **2013**, *425*, 875.
- (273) Chakraborty, A.; Wang, D.; Ebright, Y. W.; Korlann, Y.; Kortkhonjia, E.; Kim, T.; Chowdhury, S.; Wigneshweraraj, S.; Irschik, H.; Jansen, R.; Nixon, B. T.; Knight, J.; Weiss, S.; Ebright, R. H. *Science* **2012**, *337*, 591.
- (274) Revyakin, A.; Zhang, Z.; Coleman, R. A.; Li, Y.; Inouye, C.; Lucas, J. K.; Park, S. R.; Chu, S.; Tjian, R. *Genes Dev.* **2012**, *26*, 1691.
- (275) Treutlein, B.; Muschiello, A.; Andrecka, J.; Jawhari, A.; Buchen, C.; Kostrewa, D.; Hög, F.; Cramer, P.; Michaelis, J. *Mol. Cell* **2012**, *46*, 136.
- (276) Werner, F. *Trends Microbiol.* **2008**, *16*, 247.
- (277) Werner, F.; Weinzierl, R. *Mol. Cell* **2002**, *10*, 635.
- (278) Werner, F.; Weinzierl, R. O. J. *Mol. Cell. Biol.* **2005**, *25*, 8344.
- (279) Grünberg, S.; Warfield, L.; Hahn, S. *Nat. Struct. Mol. Biol.* **2012**, *19*, 788.
- (280) Hirtreiter, A.; Damsma, G. E.; Cheung, A. C. M.; Klose, D.; Grohmann, D.; Vojnic, E.; Martin, A. C. R.; Cramer, P.; Werner, F. *Nucleic Acids Res.* **2010**, *38*, 4040.
- (281) Mayer, A. A.; Heidemann, M. M.; Lidschreiber, M. M.; Schrieck, A. A.; Sun, M. M.; Hintermair, C. C.; Kremmer, E. E.; Eick, D. D.; Cramer, P. P. *Science* **2012**, *336*, 1723.
- (282) Finkelstein, I. J.; Greene, E. C. *Methods Mol. Biol.* **2011**, *745*, 447.
- (283) Wang, F.; Redding, S.; Finkelstein, I. J.; Gorman, J.; Reichman, D. R.; Greene, E. C. *Nat. Struct. Mol. Biol.* **2012**, *20*, 174.
- (284) Sanchez, A.; Osborne, M. L.; Friedman, L. J.; Kondev, J.; Gelles, J. *EMBO J.* **2011**, *30*, 3940.
- (285) Friedman, L. J.; Gelles, J. *Cell* **2012**, *148*, 679.
- (286) Larson, M. H.; Greenleaf, W. J.; Landick, R.; Block, S. M. *Cell* **2008**, *132*, 971.
- (287) Tinoco, I.; Bustamante, C. *Biophys. Chem.* **2002**, *101–102*, 513.
- (288) Keller, D.; Bustamante, C. *Biophys. J.* **2000**, *78*, 541.
- (289) Dalal, R. V.; Larson, M. H.; Neuman, K. C.; Gelles, J.; Landick, R.; Block, S. M. *Mol. Cell* **2006**, *23*, 231.
- (290) Liphardt, J.; Onoa, B.; Smith, S. B.; Tinoco, I.; Bustamante, C. *Science* **2001**, *292*, 733.
- (291) Liphardt, J.; Dumont, S.; Smith, S. B.; Tinoco, I.; Bustamante, C. *Science* **2002**, *296*, 1832.
- (292) Epshtein, V.; Dutta, D.; Wade, J.; Nudler, E. *Nature* **2010**, *463*, 245.
- (293) Kim, M.; Krogan, N. J.; Vasiljeva, L.; Rando, O. J.; Nedeja, E.; Greenblatt, J. F.; Buratowski, S. *Nature* **2004**, *432*, 517.
- (294) Luo, W.; Bentley, D. *Cell* **2004**, *119*, 911.
- (295) Tollervey, D. *Nature* **2004**, *432*, 456.
- (296) Rondon, A.; Mischo, H.; Proudfoot, N. *Nat. Struct. Mol. Biol.* **2008**, *15*, 775.
- (297) Mischo, H. E.; Proudfoot, N. J. *Biochim. Biophys. Acta, Gene Regul. Mech.* **2012**, *1*.
- (298) Kuehner, J. N.; Pearson, E. L.; Moore, C. *Nat. Rev. Mol. Cell Biol.* **2011**, *12*, 283.
- (299) Larson, D. R. *Curr. Opin. Genet. Dev.* **2011**, *21*, 591.
- (300) Raj, A.; Van Oudenaarden, A. *Annu. Rev. Biophys.* **2009**, *38*, 255.
- (301) Lionnet, T.; Singer, R. H. *EMBO Rep.* **2012**, *13*, 313.
- (302) Paré, A.; Lemons, D.; Kosman, D.; Beaver, W.; Freund, Y.; McGinnis, W. *Curr. Biol.* **2009**, *19*, 2037.
- (303) Harper, C. V.; Finkenzstädt, B.; Woodcock, D. J.; Friedrichsen, S.; Semprini, S.; Ashall, L.; Spiller, D. G.; Mullins, J. J.; Rand, D. A.; Davis, J. R. E.; White, M. R. H. *PLoS Biol.* **2011**, *9*, e1000607.
- (304) Tan, R. Z.; Van Oudenaarden, A. *Mol. Syst. Biol.* **2010**, *6*, 1.
- (305) Muramoto, T.; Müller, I.; Thomas, G.; Melvin, A.; Chubb, J. R. *Curr. Biol.* **2010**, *20*, 397.
- (306) Zenklusen, D.; Larson, D. R.; Singer, R. H. *Nat. Struct. Mol. Biol.* **2008**, *15*, 1263.
- (307) Gandhi, S. J.; Zenklusen, D.; Lionnet, T.; Singer, R. H. *Nature Publishing Group* **2010**, *18*, 27.
- (308) Karpova, T. S.; Kim, M. J.; Spriet, C.; Nalley, K.; Stasevich, T. J.; Kherrouche, Z.; Heliot, L.; McNally, J. G. *Science* **2008**, *319*, 466.
- (309) Hocine, S.; Raymond, P.; Zenklusen, D.; Chao, J. A.; Singer, R. H. *Nat. Methods* **2012**, *10*, 119.